JOURNAL OF VIROLOGY, May 2002, p. 4467–4482 Vol. 76, No. 9
0022-538X/02/$04.00+0 DOI: 10.1128/JVI.76.9.4467–4482.2002


# Gene Expression Pattern in Caco-2 Cells following Rotavirus Infection

Mariela A. Cuadras,[1] Dino A. Feigelstock,[1]† Sungwhan An,[1]‡ and Harry B. Greenberg[1,2,3]*

*Department of Medicine[1] and Department of Microbiology and Immunology,[2] Stanford University School of Medicine, Stanford, California 94305, and the VA Palo Alto Health Care System, Palo Alto, California 94304[3]*

Received 3 October 2001/Accepted 11 January 2002

**Rotaviruses are recognized as the leading cause of severe dehydrating diarrhea in infants and young children worldwide. Preventive and therapeutic strategies are urgently needed to fight this pathogen. In tissue culture and in vivo, rotavirus induces structural and functional alterations in the host cell. In order to better understand the molecular mechanisms involved in the events after rotavirus infection, we identified host cellular genes whose mRNA levels changed after infection. For this analysis, we used microarrays containing more than 38,000 human cDNAs to study the transcriptional response of the human intestinal cell line Caco-2 to rotavirus infection. We found that 508 genes were differentially regulated >2-fold at 16 h after rotavirus infection, and only one gene was similarly regulated at 1 h postinfection. Of these transcriptional changes, 73% corresponded to the upregulation of genes, with the majority of them occurring late, at 12 or more hours postinfection. Some of the regulated genes were classified according to known biological function and included genes encoding integral membrane proteins, interferon-regulated genes, transcriptional and translational regulators, and calcium metabolism-related genes. A new picture of global transcriptional regulation in the infected cell is presented and families of genes which may be involved in viral pathogenesis are discussed.**

Rotaviruses are the leading cause of severe dehydrating diarrhea in infants and young children worldwide (22, 30). Given the importance of this pathogen to human health, preventive and therapeutic strategies are urgently required. Studies directed at better understanding the host cellular events following rotavirus infection are likely to provide insights which will advance progress toward preventing and/or treating this infection.

Rotaviruses, members of the *Reoviridae* family, are nonenveloped viruses composed of 11 segments of double-stranded RNA (dsRNA) surrounded by three concentric layers of protein (15). In vivo, the virus infects the mature, differentiated enterocyte of the small intestinal epithelium (4). The majority of our knowledge about the virus replication cycle comes from studies performed in tissue culture cells, to which rotaviruses have been adapted to grow. These studies showed that the entire viral replication cycle occurs in the cytoplasm of the infected cell (reviewed in reference 15). However, little is known about the molecular mechanisms underlying the cellular response to infection. Viruses cause a variety of responses in infected cells, including changes in gene and protein expression, interferon (IFN) response, regulation of cell surface molecules, etc. A reduction in cellular protein synthesis has been reported in rotavirus-infected cells (25). Changes in intracellular $Ca^{2+}$ concentration (associated with virus maturation and proposed to be related to cell death) (41), alterations in the organization of the cell cytoskeleton (5, 28), structural and functional alterations in the tight junctions (43), and cellular lysis (15) have also been described following rotavirus infection. These phenotypic responses could be associated with alterations in mRNA expression of particular host cell genes. In addition, identification of changes in expression levels of other genes in rotavirus-infected cells can provide insights concerning the mechanisms of viral pathogenesis. Some limited attempts have been made to characterize the mRNA and protein expression levels of certain cellular genes in rotavirus-infected cells. Northern blot analysis and two-dimensional gel electrophoresis showed that, in MA104 cells infected with the SA11 strain of simian rotavirus, there is an increase in the mRNA and protein levels of two endoplasmic reticulum (ER)-resident chaperones (GRP78 and GRP94) (58). Rollo et al. (46) showed increases in the mRNA expression level of certain chemokines and IFNs in rhesus rotavirus (RRV)-infected HT-29 cells. To date, no studies have been presented that describe the global transcriptional response of cells undergoing rotavirus infection.

The emergence in the last several years of DNA microarray technology provides a powerful tool for studying the simultaneous transcriptional expression of thousands of host genes. Oligonucleotide- and cDNA-based arrays have been used to study the transcriptional responses of cells subjected to a variety of environmental stimuli, including viral infections, such as cytomegalovirus (60), human immunodeficiency virus (HIV) (21), influenza virus (20), and others (7, 42). In this work we used microarrays containing more than 38,000 human cDNAs to characterize the transcriptional response of human intestinal Caco-2 cells to RRV infection. Caco-2 cells were selected as a good cell culture model of human intestinal cells, and RRV was selected because it has been orally administered to hundreds of thousands of people as a live virus vaccine.

* Corresponding author. Mailing address: VAPAHCS, 3801 Miranda Ave., MC 154C, Palo Alto, CA 94304. Phone: (650) 493-5000, ext. 63124. Fax: (650) 852-3259. E-mail: hbgreen@leland.stanford.edu.

† Present address: Laboratory of Hepatitis and Related Emerging Agents, DETTD/OBRR/CBER/FDA, Bethesda, MD 20892.

‡ Present address: Genomictree, Inc., Daeduk BioCommunity, Jonmin-Dong 461-6, Daejon 305-390, South Korea.

## MATERIALS AND METHODS

**Cells, viruses, and infection conditions.** The human intestinal epithelial cell line Caco-2 was obtained from the American Type Culture Collection (Rockville, Md.). Cells were grown in RPMI 1640 medium with 300 mg of L-glutamine

TABLE 1. Hybridization scheme designed to analyze the transcriptional response of Caco-2 cells to RRV infection using cDNA microarrays

| Hybridization | Expt description[a] | cDNA source[b] | cDNA source[c] |
|---|---|---|---|
| 1 | Control 1 | $Mock_a$ 16 h | $Mock_b$ 16 h |
| 2 | Control 2 | $Mock_c$ 16 h | $Mock_a$ 16 h |
| 3 | Control 3 | $RRV_a$ 16 h | $RRV_b$ 16 h |
| 4 | Infection 1 | $RRV_a$ 16 h | $Mock_a$ 16 h |
| 5 | Infection 2 | $RRV_b$ 16 h | $Mock_b$ 16 h |
| 6 | Infection 3 | $RRV_b$ 16 h | $Mock_a$ 16 h |
| 7 | Control 4 | $Mock_a$ 1 h | $Mock_b$ 1 h |
| 8 | Control 5 | $Mock_c$ 1 h | $Mock_a$ 1 h |
| 9 | Infection 4 | $RRV_a$ 1 h | $Mock_a$ 1 h |
| 10 | Infection 5 | $RRV_b$ 1 h | $Mock_b$ 1 h |
| 11 | Infection 6 | $RRV_b$ 1 h | $Mock_a$ 1 h |

[a] As was assigned for each microarray.
[b] Fluorescently labeled with red dye during the RT reaction.
[c] Fluorescently labeled with green dye during the RT reaction.

(BioWhittaker, Walkersville, Md.)/liter, supplemented with 100 IU of penicillin-streptomycin (BioWhittaker)/ml and 15% fetal bovine serum (FBS; Gibco-BRL, Gaithersburg, Md.). Fresh medium was replaced approximately every 10 days. The rhesus monkey epithelial cell line MA104 was grown in Medium 199 with Earle's balanced salt solution, 2.2 g of $NaHCO_3$/liter, and 100 mg of L-glutamine (BioWhittaker)/liter, supplemented with 100 IU of penicillin and streptomycin/ml and 10% FBS. Cell cultures and viral infections were kept in a 5% $CO_2$ incubator at 37°C.

Rhesus rotavirus (RRV) was propagated as follows: monolayers of MA104 cells were infected with 1 focus-forming unit (FFU) per cell of trypsin (10 μg/ml)-activated RRV in the absence of FBS. Viral lysates were harvested when substantial cytopatic effect was observed (18 to 24 hours postinfection [hpi]) by freezing and thawing two times. The lysates were cleared by centrifugation at 3,000 rpm in a tabletop Allegra 6R Centrifuge (Beckman Coulter, Fullerton, Calif.) at 4°C for 10 min. Virus titers were determined in monolayers of Caco-2 cells by an FFU assay as described elsewhere (37), and aliquots of this lysate were stored at −80°C.

For microarray experiments Caco-2 cells (passages 27 to 36) were seeded in 175-$cm^2$ tissue culture flasks (Falcon; Becton Dickinson, Franklin Lakes, N.J.). At 17 to 26 days postseeding, the cells were washed twice with RPMI medium and then infected at a multiplicity of infection (MOI) of 20 FFU of trypsin-activated RRV in a final volume of 25 ml of medium without FBS. After 1 h at 37°C, the inoculum was removed, the monolayers were washed once with medium, and the cells were harvested or incubated for an additional period of 15 h. At the end of each incubation, the cells were washed twice with phosphate-buffered saline (PBS), and 8 ml of RNAwiz (Ambion, Austin, Tex.) were added to the flask for extraction of total RNA. As a reference, mock-infected Caco-2 cells were treated under the same conditions as infected cells except that the "mock" inoculum was derived from a cleared lysate of uninfected MA104 cells.

The microarray experiments reported in this work were performed as follows. The first set of comparisons consisted of two separate RRV infections ($RRV_a$ and $RRV_b$) and three separate mock infections ($mock_a$, $mock_b$, and $mock_c$) for each time point (1 and 16 hpi). A total of 11 different hybridization combinations were made (Table 1). In this analysis we made three separate comparisons of rotavirus-infected cells to mock-infected cells as described in Table 1. The second set of comparisons were a time course experiment (Fig. 5), which consisted of four separate RRV infections that were harvested at 1, 6, 12, and 24 hpi and five separate mock infections that were harvested at the 1, 2, 6, 12, and 24 h time points. A total of five different hybridizations were made (mock 2 h versus mock 2 h as a control comparison, RRV 1 h versus mock 1 h, RRV 6 h versus mock 6 h, RRV 12 h versus mock 12 h, and RRV 24 h versus mock 24 h).

**mRNA isolation, preparation of fluorescently labeled cDNA, and hybridization.** Total RNA was extracted by using RNAwiz according to the manufacturer's protocol. After RNA extraction, poly(A) mRNA was purified with the FastTrack 2.0 kit (Invitrogen, Carlsbad, Calif.) according to the manufacturer's instructions for the isolation of mRNA starting from total RNA. The concentration of mRNA was determined by measuring the absorbance at 260 nm.

For analysis of rotavirus infection versus mock infection, fluorescently labeled cDNA from rotavirus-infected cells was generated by reverse transcription (RT) by using the red fluorescent dye Cy5 (Amersham Pharmacia, Piscataway, N.J.); fluorescent cDNA from mock-infected cells was prepared by using the green fluorescent dye Cy3 (Amersham Pharmacia). For control comparisons (mock versus mock and RRV versus RRV), cDNA from mock- or RRV-infected cells was generated and fluorescently labeled during a RT reaction with Cy5 or Cy3 (see Table 1). For each RT reaction, 3 μg of poly(A) mRNA was mixed with 2 μg of an achored oligo(dT) primer (MWG-Biotech, High Point, N.C.) in a total volume of 15 μl, heated for 10 min at 72°C, and transferred to ice. Then, the RT mix (6 μl of 5× first-strand buffer [Gibco-BRL], 3 μl of 0.1 M dithiothreitol, 0.6 μl of unlabeled nucleotides [25 mM concentrations each of dCTP, dGTP, and dATP and 15 mM dTTP; Boehringer Mannheim, Indianapolis, Ind.], 3 μl of either Cy5-dUTP or Cy3-dUTP [catalog numbers PA53021 or PA53022, respectively], and 2 μl of Superscript II reverse transcriptase [Gibco-BRL]) was added in a final reaction volume of 30 μl. The reaction was incubated for 2 h at 42°C, and 15 μl of 0.1 N NaOH was added to degrade the RNA (10 min at 72°C). The mix was neutralized by addition of 15 μl of 0.1 N HCl; at this time the two cDNAs (Cy5 and Cy3 labeled) were mixed, and the final volume was increased to 500 μl with TE (10 mM Tris, pH 8.0; 1 mM EDTA). The mixed cDNAs were extracted with 500 μl of buffer saturated phenol-chloroform-isoamyl alcohol (25:24:1 [vol/vol/vol]; Gibco-BRL), and the aqueous phase was transferred to a Microcon YM-30 (Amicon Millipore, Bedford, Mass.), centrifuged for 10 min at 10,000 rpm in a benchtop Eppendorf 5415C centrifuge, and washed with 400 μl of TE. Next, 20 μg of Cot1 human DNA (Gibco-BRL), 20 μg of poly(A) RNA (Sigma), and 20 μg of tRNA (Gibco-BRL) were added, and the mixture was concentrated to 40 μl. For final probe preparation, 8 μl of 20× SSC (1× SSC is 0.15 M NaCl plus 0.015 M sodium citrate) and 4 μl of 3.3% sodium dodecyl sulfate (SDS) were added, the mixture was denaturated for 2 min at 93°C, incubated for 20 min at room temperature, and transferred to the microarray surface. The microarray and probe were covered with a 22-by-60-mm glass coverslip and incubated overnight at 65°C in custom-made slide chambers maintaining the humidity with a few drops of 3× SSC. After hybridization, the arrays were transferred to a glass slide-rack and washed with 1× SSC–0.03% SDS until the coverslips were removed, and then two additional washes of 2 min each with gentle agitation were performed in increasing stringency solutions (0.2× and 0.05× SSC). The arrays were dried at room temperature by centrifugation for 5 min at 500 rpm in the Allegra 6R tabletop centrifuge.

The cDNA microarrays used in this work were produced in the Microarray Production Facility of Stanford University, and the protocols for their production have been described elsewhere (27, 48). These arrays contain 39,552 array elements, of which 38,432 correspond to human sequence verified genes, 447 correspond to nonhuman genes, and 673 correspond to unknown samples. Detailed protocols for the array production are available online (http://cmgm.stanford.edu/pbrown/).

**Signal detection and data analysis.** The fluorescent intensity for each dye was detected by using a GenePix 4000b microarray scanner (Axon Instruments, Foster City, Calif.). Images were analyzed by using the GenePix Pro 3.0 software provided with the scanner. First, each spot was defined automatically by a spot-indicator (grid). The software automatically discards (flags) a spot (i) if the intensity is not greater than the background threshold, (ii) if the spot has an irregular size, or (iii) if the grid designed to that spot overlaps with an adjacent grid (see the GenePix Pro 3.0 user's manual for more details). After the automatic gridding and flagging, a visual inspection was performed to eliminate from the analysis all spots with signals due to visually detectable array artifacts. GenePix Pro 3.0 displays the data in tables that can be exported in any standard spreadsheet program.

The data files generated by the software were entered into the Stanford Microarray Database (SMD), a custom database that maintains Web-accessible files for further analysis (52). After submission into SMD, the red signal was normalized by applying a single multiplicative factor to all intensities measured for the red dye Cy5. The normalization factor was computed so that the median Cy3/Cy5 fluorescent ratio of nonflagged spots on each array was 1.0.

To reduce the effect of nonspecific fluorescence, we filtered all nonflagged spots as follows. First, the mean background for the red and green signal in each array was determined by calculating the average of the median background of the corresponding color from all nonflagged spots in the array. Then, this mean background plus three standard deviations was established as our threshold intensity value for each color. In addition, the mean intensity of one of the colors per spot was required to be at least two times greater than its local background. Genes whose spot intensities did not pass these filter criteria were eliminated from further analysis. Based on these filter criteria, between 20,093 and 24,926 of arrayed human genes were eliminated from our analysis.

To analyze levels of up- or downregulation, we applied a hierarchical clustering algorithm implemented by the software Cluster as described by Eisen et al. (14). This software clusters genes according to their similarity in the pattern of gene expression and displays the data in a dendrogram that resembles a tree

(TreeView). Each row represents genes, and each column represents a single experiment or microarray. In this TreeView image the computed red/green ratios for each spot are represented by color display, black cells represent red/green ratios of 1.0 (unchanged genes), red cells represent ratios with increasing intensities of red (upregulated genes), and green cells represent ratios with increasing intensities of green (downregulated genes). A detailed explanation of the Cluster and TreeView is presented by Eisen et al. (14), and this software is available online (http://rana.stanford.edu/software).

The selection criteria for identification of genes that were up- or downregulated by the rotaviral infection are described in relation to each data set in the result section.

**Measurement of cell viability and the percentage of infected cells.** Caco-2 cell viability was determined by using the LIVE/DEAD Viability/Cytotoxicity Kit for animal cells (Molecular Probes, Eugene, Oreg.) according to the manufacturer's instructions for flow cytometry analysis. Briefly, confluent monolayers of Caco-2 cells in six-well plates were or were not infected at an MOI of 30 FFUs with trypsin-activated RRV. After 16 h of infection, the cells were washed three times with PBS and detached by incubation in 0.05% trypsin–0.53 mM EDTA (Gibco-BRL). After trypsinization, the cells were transferred to a tube, pelleted by centrifugation (500 × *g*), and washed twice with PBS. As a positive control for dead cells, half of the cells were killed by permeabilization in 70% methanol-PBS for 20 min at room temperature. Then, cells were resuspended in 400 μl of 1 μM calcein AM and 2 μM ethidium homodimer (EthD-1) in PBS and incubated for 15 min at room temperature. After incubation, the fluorescent signal was analyzed by using a FACScan flow cytometer and CellQuest software (Becton Dickinson) with appropriate gating parameters.

For quantification of the percentage of infected cells, cells were mock or RRV infected as described above. After trypsinization, cells were fixed in 10% formalin in PBS for 30 min at room temperature and then permeabilized for 3 min in 1% Triton X-100 in PBS at room temperature. The cells were washed twice with PBS and then incubated in a 1:500 dilution of a rabbit polyclonal hyperimmune serum to RRV in PBS for 30 min at 4°C, washed twice with PBS, and then incubated with a 1:100 dilution of fluorescein-conjugated anti-rabbit immunoglobulin G (Kirkegaard & Perry, Gaithersburg, Md.) in PBS for 30 min at 4°C. After the incubation period, the number of antibody binding cells was determined by flow cytometry with the instrumentation described above.

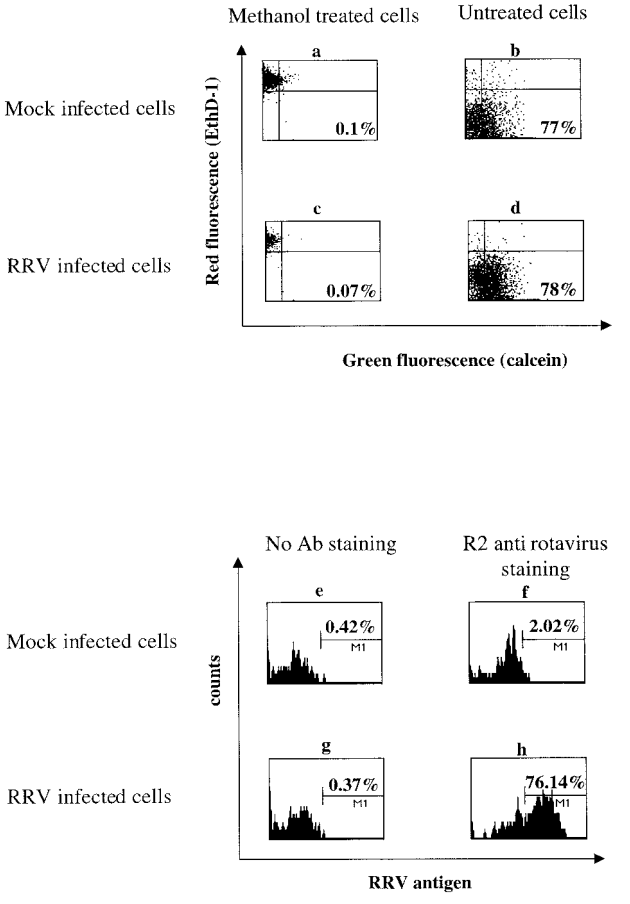


FIG. 1. (a to d) Viability of Caco-2 cells 16 h after rotavirus infection. Caco-2 cells were grown as monolayers and, at 15 days postseeding, were mock (a and b) or RRV (c and d) infected at an MOI of 30. At 16 hpi the cell viability was assessed by measuring the percentage of live and dead cells by FACS analysis. Live cells were identified by the presence of intracellular esterase activity, which was detected by treating the cells with calcein-AM. Dead cells were identified by measuring membrane damage, which was detected by treating the cells with ethidium homodimer (EthD-1). A fraction of the cells (a and c) were killed by permeabilization with 70% methanol for 20 min, as positive control for dead cells. (e to h) A percentage of cells were infected with RRV. Caco-2 cells were grown as monolayers and, at 15 days postseeding, were mock (e and f) or RRV (g and h) infected at an MOI of 20. At 16 hpi the cells were permeabilized, stained with a rabbit polyclonal anti-rotavirus serum (f and h) or mock stained (e and g), further stained with an anti-rabbit FITC-conjugated immunoglobulin, and subjected to FACS analysis.

## RESULTS

**Viability of RRV-infected Caco-2 cells and evaluation of the percentage of cells infected.** We used human cDNA microarrays to study the global transcriptional response of cells infected with rotavirus. We chose the human intestinal cell line Caco-2 (16) as a model that would mimic characteristics of rotavirus replication in vivo. Caco-2 cells were derived from a human colon adenocarcinoma and display several characteristics of mature enterocytes, such as cellular polarization, development of an apical brush border membrane, and expression of intestinal hydrolases on the apical domain (62). In addition, Caco-2 cells have been used to study the interaction of several enteropathogens with the intestine (39, 40, 54), and most rotavirus strains, including our laboratory strain RRV, grow efficiently in Caco-2 cells (32, 55).

We choose 16 h as a primary time point to evaluate the cellular transcriptional response to rotavirus infection because Caco-2 cells are lysed at late times after infection (after 24 to 48 h) (29, 43). To establish the viability of the cells at 16 hpi under our experimental conditions, Caco-2 cells were grown in monolayers and, 15 days postseeding, were mock or RRV infected at an MOI of 30. At 16 hpi cellular viability was assessed by measuring the percentage of live and dead cells, as described in Materials and Methods. A fraction of the cells were killed by permeabilization with 70% methanol for 20 min and used as a positive control for dead cells. The percentage of living cells was determined by the presence of intracellular esterase activity which was detected by measuring the conversion of calcein AM to calcein by fluorescence-activated cell sorting (FACS) analysis. The percentage of dead cells was determined by membrane damage, which was detected by measuring the binding of ethidium homodimer (EthD-1, an impermeable fluorescent dye) to nucleic acids by FACS analysis (Molecular Probes Live/Dead Viability/Cytotoxicity Kit, L-3224). As can be seen in Fig. 1b and d, mock- and RRV-infected cells look similar at 16 hpi; 77% of the mock-infected and 78% of the RRV-infected cells were positive for intracellular esterase activity and negative for EthD-1 staining (lower right quadrant). In contrast, >97% of the methanol treated cells were positive for EthD-1 and negative for calcein staining (upper left quadrant, Fig. 1a and c). Taken together, these

results indicate that at 16 h after rotavirus infection Caco-2 cells were alive.

We also determined the percentage of cells infected under our conditions. Caco-2 cells were mock or RRV infected at an MOI of 20; at 16 hpi the cells were fixed and stained with a rabbit polyclonal antiserum against RRV as described in Materials and Methods and subjected to FACS analysis. As can be seen in Fig. 1e to h, >75% of the inoculated cells stained positively for RRV antigen. Hence, mRNA from infected cells used for hybridization analysis was derived from a population of living cells in which >75% were infected. Infection with MOIs of 50 and 100 only produced a 5% increment in the percentage of infected cells (data not shown).

**Rotavirus infection induces changes in cellular gene expression of Caco-2 cells.** Our approach for studying the cellular transcriptional response during rotavirus infection consisted of comparing the relative abundance of specific poly(A) mRNA in infected cells to the same specific poly(A) mRNA from mock-infected cells by using cDNA microarrays containing thousands of cellular genes (see Materials and Methods). Preliminary experiments with Caco-2 cells from different passage levels or different flasks at the same passage level under the same culture conditions showed some variability in the pattern of mRNA expression (data not shown). In order to specifically attribute transcriptional changes to virus infection (and not to background variability), we determined the background transcriptional variability of our cell culture system. To do this, we compared mock-infected cells versus mock-infected cells at 1 hpi, mock-infected cells versus mock-infected cells at 16 hpi, and RRV-infected cells versus RRV-infected cells at 16 hpi Each comparison was repeated one or two times (see Table 1). Representative plots of some of these comparisons are shown in Fig. 2.

We analyzed the number and percentage of gene transcripts that varied by >2-fold in this series of comparisons in order to identify the background rate of transcriptional variation in our system. As can be seen (Fig. 2a and c), when mock-infected cells were compared to mock-infected cells (at 1 and 16 h) and RRV-infected cells were compared to RRV-infected cells at 16 hpi (Fig. 2e), few transcripts varied by >2-fold: the results were 0.9, 1.15, 1.68, 1.71, and 2.2% for the five control hybridizations presented in Table 1. This variability could be due to the variability in the microarray technique (extraction and purification of the mRNA, cDNA synthesis and labeling, hybridization and/or signal detection) or to natural transcriptional variability that may occur in Caco-2 cells in culture. When we compared RRV-infected cells versus mock-infected cells at 1 hpi (Fig. 2b), 1.0, 1.2, and 1.8% of the genes varied >2-fold (for the three RRV versus mock hybridizations in Table 1), a finding which was similar to the background rate. However, when we compared RRV-infected cells versus mock-infected cells at 16 hpi, 8.6, 8.9, and 11% (for the three RRV versus mock hybridizations in Table 1) of the gene transcripts varied >2-fold (Fig. 2d). These results indicate that rotavirus infection induces changes in cellular gene expression at 16 h after infection.

**Genes that respond to RRV infection.** It was clear from our analysis (Fig. 2a and c) that there is an intrinsic variability in our cell culture system, since there were some changes in cellular gene expression that were detected when we compared RNA extractions from cells treated identically. In order to identify genes that specifically responded to RRV infection, we performed independent infections with corresponding independent controls (see Materials and Methods and Table 1).

We undertook a series of steps to identify genes that responded specifically to RRV infection. First, we selected genes that passed the filter criteria (see Materials and Methods) and did not change by >1.4-fold in control comparisons (mock versus mock and infection versus infection; Table 1). We then determined how many of these genes passed the filter criteria in the experimental comparisons (RRV versus mock) at 1 and 16 h and how many of these were up- or downregulated.

Between 35.1 and 47.7% of the human printed array elements (13,506 to 18,339 of 38,432 human printed elements) were suitable for analysis after initial filtration. After the elimination of genes that varied by ≥1.4-fold in the control comparisons, we identified a list of 8,528 genes for the 1 h time point and 9,171 genes for the 16 h time point that were suitable for further study. These genes were analyzed in the infectious comparisons (RRV versus mock). Of the 8,528 genes, 7,263 gave a signal above background in the 1-h infection comparisons (RRV versus mock) and, of the 9,171 genes from the 16 h time point, 8,575 gave a signal above the background in the 16-h infection comparisons (RRV versus mock).

A similar analysis with the nonhuman genes (the arrays contain 448 nonhuman genes from yeast and bacteria, see Materials and Methods) was also performed. Only one gene (0.22%) passed the filter criteria in 50% of the 11 arrays examined.

We used the following rationale to select the threshold for classifying genes as up- or downregulated. First, we wanted to ensure that genes identified were actually regulated by infection and, for this purpose, the higher the fold change selected as a threshold, the higher the likelihood of significance. However, we do not yet know what significance to assign to lower-level changes in transcription. Therefore, we arbitrarily chose to classify genes whose transcriptional level changed by >2-fold in at least two of the three experimental hybridizations (Table 1) as rotavirus-regulated genes. Responses of ≥2-fold have also been used as selection criteria by others to identify transcriptionally regulated genes by microarray analysis (7, 20, 27). As described above, none of the selected genes varied by >1.4-fold in any of the control comparisons.

Five hundred and eight genes were up- or downregulated by >2-fold at 16 hpi (Fig. 3). A similar analysis at the 1 h time point disclosed only one gene which changed by >2-fold (the potassium large conductance $Ca^{2+}$-activated channel). Several observations can be made from this analysis. It is clear that after 1 h of rotavirus infection, Caco-2 cells showed a very limited transcriptional response to infection (only one gene was transcriptionaly regulated >2-fold). In contrast, at 16 hpi, 579 array elements, representing 511 genes (some genes were printed more than once) were up- or downregulated. Of these, 375 (73.4%) were upregulated and 133 (26.02%) were downregulated. Of the 579 array elements identified, only three (0.58%) gave inconsistent results, being upregulated in one hybridization, and downregulated in the other hybridization. Of note, the fluorochrome signal used for labeling did not affect the results, since labeling the cDNAs in the opposite way (cDNA from mock-infected cells labeled with Cy5 and cDNA

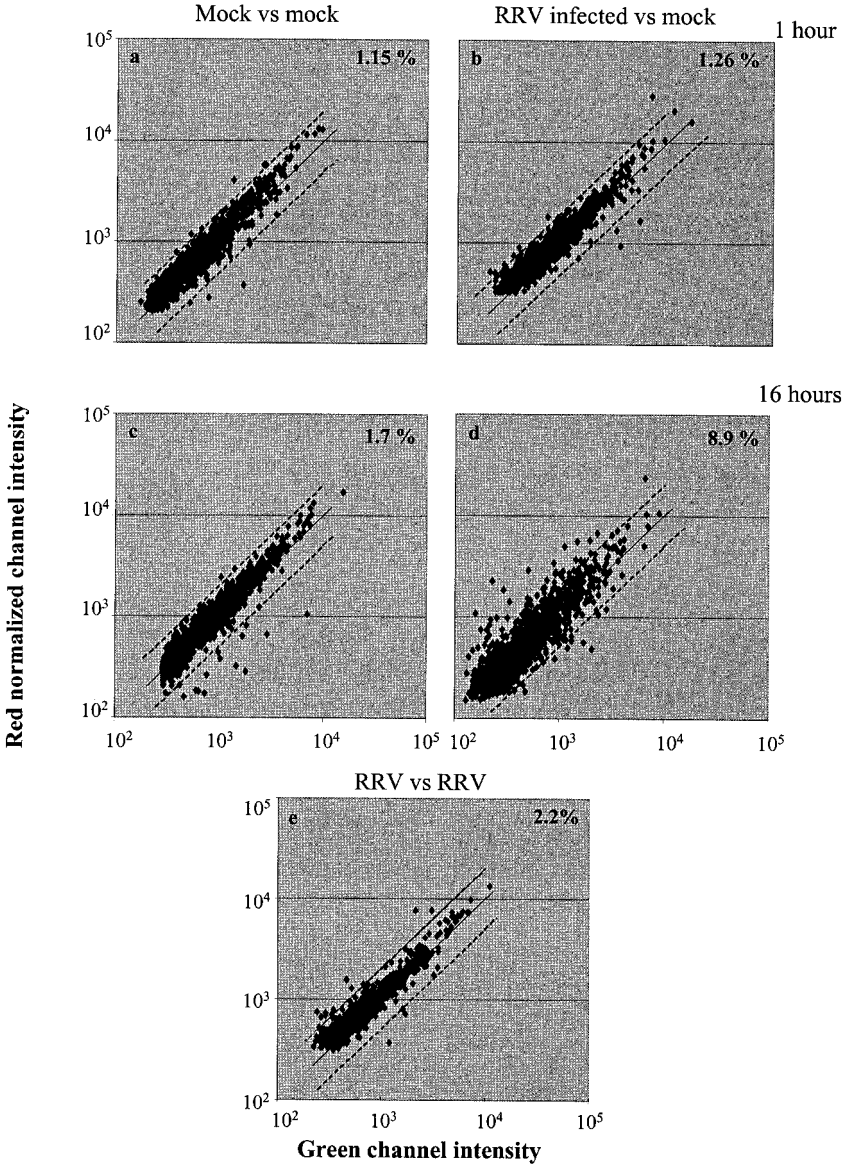


FIG. 2. Hybridization results from mock-infected cells versus mock-infected cells (a and c), RRV-infected cells versus RRV-infected cells (e), and RRV-infected cells versus mock-infected cells (b and d) at 1 hpi (a and b) and 16 hpi (c, d, and e). The *x* and *y* axes represent the intensity for the green fluorescent dye Cy3 and the normalized intensity of the red fluorescent dye Cy5, respectively. The solid lines represent no change in the level of gene expression, and the dashed lines indicate a twofold change in the transcriptional response. The percentage of genes that changed more than twofold is indicated for each panel.

from RRV-infected cells with Cy3) had very little effect (data not shown). The 579 array elements that passed the twofold change criteria represent 6.7% of the total analyzable population (8,575 genes).

An examination of the genes in Fig. 3 shows variation in the intensities of the green and red signals obtained. This reflects different levels of up- and downregulation among the various genes. We analyzed the level of change by identifying the genes that changed their level of expression between 2- and 4-fold and those that changed by >4-fold at 16 hpi. It is clear that changes between 2- and 4-fold are most frequent (Fig. 4); 463 genes were regulated between 2- and 4-fold, and only 45 genes were regulated >4-fold. Of these, 42 were upregulated, and 3 were downregulated.

The results observed were consistent across infection comparisons by using several types of analysis. The regulated genes were initially identified by setting the program to select genes that were up- or downregulated >2-fold in at least two of the three experimental hybridizations (Table 1). However, 304 of the 576 array elements (52%) or 266 of the 508 genes were regulated >2-fold in all three experimental hybridizations (hybridizations 4, 5, and 6; Table 1) and, of the remaining array elements (272), 180 were regulated >1.6-fold in the third hybridization. This means that 84% of the genes showed the same transcriptional regulation in the three separate hybridizations (hybridizations 4, 5, and 6, Table 1). Of the remaining 16% genes, half were not analyzable in the third hybridization. Only three genes (<0.04% of the total analyzed population)

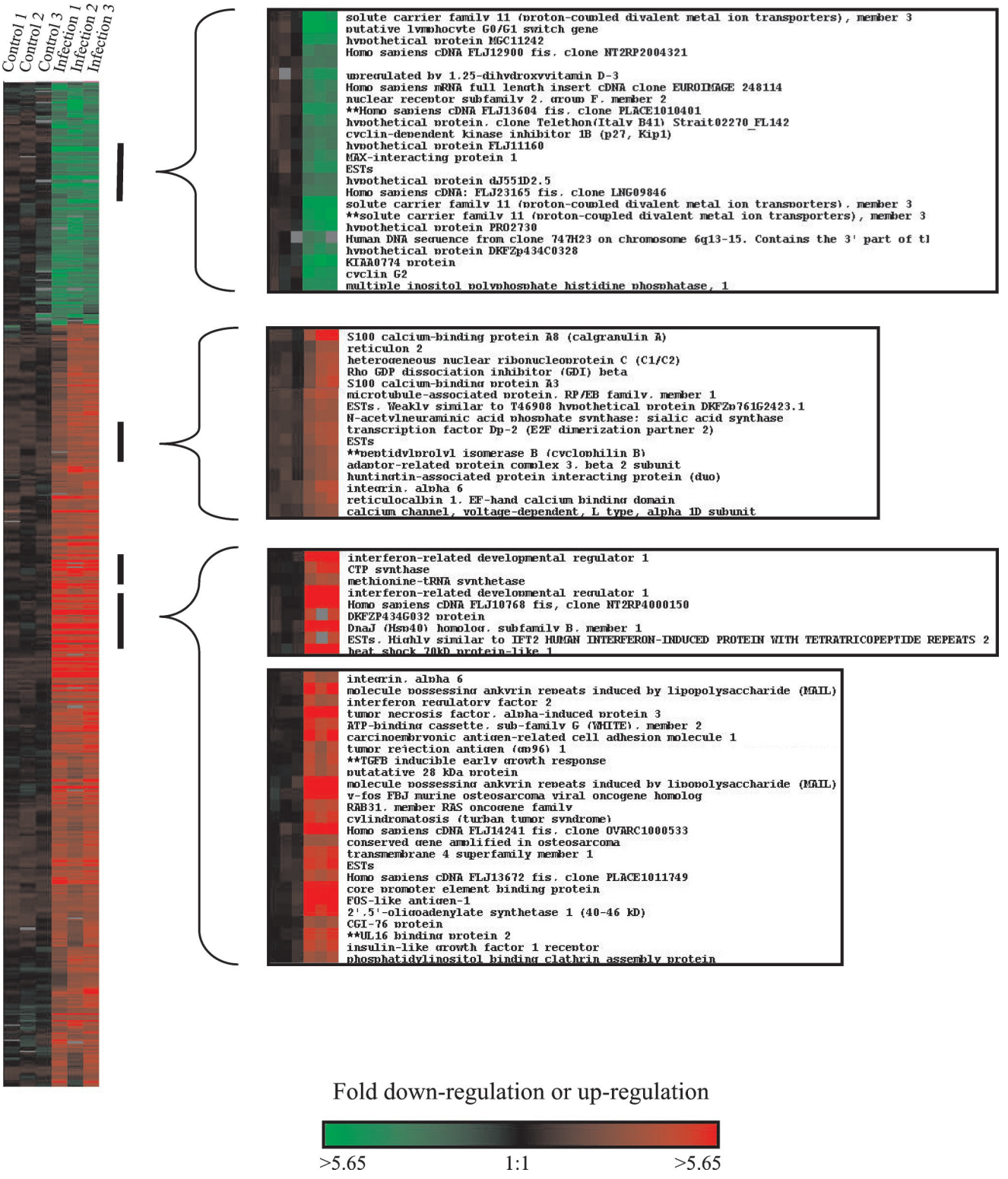


FIG. 3. Cluster analysis of genes that were differentially expressed after 16 h of RRV infection. Each horizontal row represents a single cDNA, and each vertical column represents a single microarray hybridization. The results are presented in color display; each square represents the ratio of hybridization signal of labeled cDNA prepared from the mRNA of RRV-infected or mock-infected cells relative to mock-infected cells. Red squares denote upregulated genes, green squares denote downregulation, black squares denote no significant change in the level of gene expression, and gray squares denote missing data. The colored scale for the level of up- or downregulation is depicted at the bottom. The first three columns correspond to control hybridizations (mock infected versus mock infected or RRV infected versus RRV infected), and the last three columns correspond to experimental hybridizations (RRV infected versus mock infected). The genes shown are those whose transcript levels varied >2-fold in at least two of the three experimental comparisons. Some regions are amplified at the right to show the name and the expression profile of selected genes.

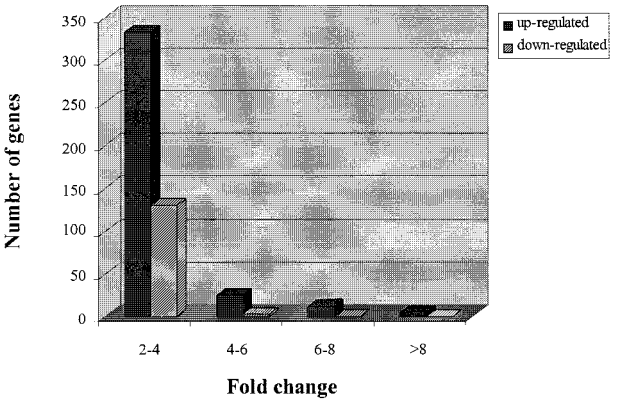


FIG. 4. Different level of gene transcription in Caco-2 cells 16 h after RRV infection. Up- or downregulated genes were classified according to their level of transcription. The categories indicated start from genes that changed between 2- and 4-fold and finish with genes that changed >8-fold. The fold change is the normalized red intensity/green intensity ratio. This ratio represents the abundance of transcript in infected cells relative to mock-infected cells at 16 hpi. For downregulated genes, the corresponding red/green ratio is the reciprocal of the fold change indicated.

showed inconsistent regulation, indicating upregulation in one experimental hybridization and downregulation in the other. From this initial analysis we conclude that rotavirus infection induces changes in the levels of 6.7% of the cellular analyzable genes in Caco-2 cells at 16 hpi, and the majority of these transcriptional responses correspond to upregulation of genes.

**The majority of the changes in cellular gene expression occur at late time points after infection.** The results of the microarray analysis at 1 and 16 hpi showed a significant difference in the transcriptional response between the two time points, from one gene at 1 hpi to 508 genes at 16 hpi. To determine whether the genes responding at 16 h were regulated at earlier times during infection, we carried out an additional time course experiment in which mock- or RRV-infected Caco-2 cells were harvested at 1, 6, 12, and 24 h after infection. Labeled cDNAs synthesized from mRNA from RRV-infected cells at each time point were mixed with labeled cDNAs synthesized from mRNA from mock-infected cells at the corresponding time points (RRV 1 h versus mock 1 h, RRV 6 h versus mock 6 h, etc.). We also carried out control comparisons by mixing labeled cDNAs from mock-infected cells with labeled cDNAs from the same batch of mock-infected cells (mock versus mock hybridization). The mixed cDNAs were hybridized to microarrays and analyzed as in the first series of hybridizations (Table 1), the difference being that in the time course experiment, we used only one infection sample and one mock-infected sample for each time point.

We focused our analysis on the genes that were regulated by >2-fold in the first experiment (Fig. 3 and Table 3) at 16 hpi to find out whether the changes observed at 16 hpi could be detected at earlier time points. We eliminated genes that changed their level of expression by 1.4-fold or more in the control comparison of the time course experiment. We next selected 227 genes that passed the filtering criteria (described in Materials and Methods) for all time points (i.e., control and 1, 6, 12, and 24 h). Cluster analysis was then performed with the five hybridizations of the time course experiments and one (RRV versus control) hybridization from the 16-h time point. Figure 5 shows the pattern of expression for selected genes that were up- or downregulated >2-fold in at least two hybridizations in the time course analysis. A common pattern was found in the time course study; the number of up- and downregulated genes increased with the time from infection, starting with very few genes after 1 h and reaching the maximum at the latest time points (16 and 24 hpi). In the time course experiment, up- and downregulated genes were observed, and again upregulated genes were most frequent (Fig. 5). Of 227 genes examined, 3 were transcriptionally regulated (>2-fold change) at 6 hpi and 33 genes were transcriptionally regulated at 12 hpi (Table 2). It is clear from these results that most of the responses observed at 16 hpi in the first experiment (Fig. 3, Table 1) became detectable late, i.e., at 12 hpi or later.

**Grouping of genes according to their biological function.** We identified 375 upregulated and 133 downregulated genes following rotavirus infection in our primary analysis. A complete list of these genes is presented in Table 3. In an attempt to facilitate the analysis of our data, we grouped the differentially regulated genes according to known biological functions. However, the classification of genes to specific cellular functions is difficult because many genes participate in more than one biological process. We listed the regulated genes in only a single functional category for simplicity. Only two genes listed in Table 3 have been previously described as rotavirus-induced genes (endoplasmin and RANTES). The regulation of some genes involved in calcium homeostasis, cytoskeleton structure, IFN regulation, and stress response were anticipated since previous data demonstrated the relationship between rotavirus infection and these biological processes (5, 6, 11, 44, 46, 58). Genes associated with other important cell functions, including cell cycle and proliferation, protein degradation, viral receptors, and membrane transporters are also regulated in response to rotavirus infection (Table 3).

## DISCUSSION

We investigated the transcriptional changes in Caco-2 cells after RRV infection in order to better understand the cell response to this important enteric pathogen. We used Caco-2 cells as a host cell to try to mimic characteristics of rotavirus replication in the human gut. We used an animal strain of rotavirus, RRV, because this strain replicates well in tissue-cultured cells and because RRV has been given to many hundreds of thousands of people in the form of a live attenuated vaccine. Human strains of rotavirus do not replicate as well as many animal strains in cell culture. Given that Caco-2 cells are lysed late after infection (29, 43), we performed our analysis of the cellular transcriptional response at 1 and 16 hpi as early and intermediate time points in the replication cycle. We also analyzed the transcriptional response over a broader time course of infection (1, 6, 12, and 24 hpi).

We learned that there are changes in the amount of mRNA transcripts present in RRV-infected Caco-2 cells compared to mock-infected cells, with 576 of 8,575 analyzable array elements changing by >2-fold at 16 hpi. These changes involve both the upregulation and the downregulation of specific gene transcripts, with a majority of the changes being upregulation. The majority of the changes occurred at times at or after 12 h


FIG. 5. Cluster analysis of selected genes that were significantly up- or downregulated at 16 hpi during a time course of rotavirus infection. An array from the 16-h time point of the first experiment is included for comparison. Genes that passed filtering criteria in all of the hybridizations and were not regulated by >1.4-fold in the control hybridization were studied. Of the selected genes, genes that were regulated by >2-fold in at least two arrays are shown. The color coding is the same as in Fig. 3.

TABLE 2. Genes up- or downregulated by >2-fold at 6 and/or 12 h after rotavirus infection (from the 508 genes that were regulated at 16 hpi)

| Time postinfection (h) and gene | Fold change[a] |
|---|---|
| 6 | |
| ESTs[b] | 0.5 |
| Tax interaction protein 1 | 2.08 |
| Nucleolar protein p40; homolog of EBNA1-binding protein | 2.12 |
| 12 | |
| Nuclear receptor subfamily 2, group F, member 2 | 0.32 |
| *Homo sapiens* mRNA; cDNA DKFZp586F1322 | 0.38 |
| Hypothetical protein DKFZp566G1424 | 0.39 |
| Human DNA sequence from clone 747H23 on chromosome 6q13-15 | 0.37 |
| *Homo sapiens* cDNA: FLJ21278 fis, clone COL01832 | 0.48 |
| Alpha-methylacyl-coenzyme A racemase | 0.39 |
| *Homo sapiens* cDNA FLJ13604 fis, clone PLACE1010401 | 0.48 |
| Cyclin-dependent kinase inhibitor 1B (p27, Kip1) | 0.41 |
| Epidermal growth factor receptor (avian erythroblastic leukemia viral (v-erb-b) oncogene homolog) | 2.02 |
| ESTs | 2.18 |
| Cartilage linking protein 1 | 2.35 |
| Steroid-5-alpha-reductase, alpha-polypeptide 1 (3-oxo-5-alpha-steroid-delta-4-dehydrogenase-alpha-1) | 2.71 |
| *Homo sapiens* cDNA FLJ20153 fis, clone COL08656 | 2.58 |
| Putative *b, b*-carotene-9′,10′-dioxygenase | 2.53 |
| Thioredoxin reductase 1 | 2.87 |
| Splicing factor, arginine/serine-rich 3 | 2.14 |
| Molecule possessing ankyrin repeats induced by lipopolysaccharide (MAIL), homolog of mouse | 4.76 |
| IFN-related developmental regulator 1 | 2.18 |
| Nuclear factor kappa, light polypeptide | 2.04 |
| v-fos FBJ murine osteosarcoma viral oncogene homolog | 15.6 |
| Chromosome 21 open reading frame 50 | 3.67 |
| Protein kinase H1l; small stress protein-like protein HSP22 | 2.04 |
| Heat shock 70-kDa protein-like 1 | 2.57 |
| Caveolin 2 | 2.10 |
| v-jun avian sarcoma virus 17 oncogene homolog | 4.9 |
| Arginine-rich, mutated in early-stage tumors | 2.76 |
| Solute carrier family 3 (activators of dibasic and neutral amino acid transport), member 2 | 2.52 |
| KIAA0005 gene product | 2.33 |
| E74-like factor 3 | 2.23 |
| Serum-inducible kinase | 2.41 |
| Ectodermal-neural cortex (with BTB-like domain) | 2.03 |
| Eukaryotic translation initiation factor 2B, subunit 2 (beta, 39 kDa) | 2.18 |
| Transgelin | 2.78 |

[a] Values of >2 and <0.5 correspond to up- and downregulated genes, respectively.
[b] ESTs, expressed sequence tags.

of infection, with an increasing number of genes identified as infection proceeded. Among the upregulated genes, we found different levels of regulation with most genes changing between 2- and 4-fold, and only 42 genes being upregulated by >4-fold in our analysis. Rotavirus infection regulates the expression of a number of genes with related functions, including genes coding for cellular structural proteins, stress-related proteins, IFN-related genes, $Ca^{2+}$-related proteins, and transcriptional and translational regulators. In addition, many genes previously unknown to be related to rotavirus or other viral infections were found to be modulated.

One of our concerns was to optimize our ability to identify genes regulated by rotavirus infection as opposed to other causes of transcriptional variation under our experimental conditions. Variability due to mRNA extraction and purification, cDNA synthesis, labeling and purification, and signal detection could generate changes in the amount of mRNA detected. Also, natural transcriptional variation is likely to occur in Caco-2 cells during culture. An analysis of the sources of background transcriptional variability was not carried out in our studies. We did, however, utilize a variety of strategies to minimize background variability. We used duplicate or triplicate assays for each condition tested. For example, two sets of flasks were infected with RRV and harvested at 16 hpi, and mRNA from each set of flasks was extracted and tested separately and compared to three separate control flasks. Fluorescently labeled cDNAs were synthesized by using each separate extracted mRNA. In this way we obtained independent samples of fluorescently labeled cDNAs from RRV-infected cells. In the same way, we obtained three samples of fluorecently labeled cDNAs from mock-infected cells. These cDNAs were mixed by using different combinations (mock versus mock, RRV versus RRV, and RRV versus mock; Table 1) and hybridized to microarrays in order to increase the number of replicate experiments analyzed.

The analysis of the control arrays (mock versus mock and RRV versus RRV; Fig. 2 and results not shown) identified genes that were variable under similar experimental conditions. We used this information to eliminate from the analysis any transcript demonstrating a ≥1.4-fold change in at least one of these control hybridizations. This procedure assumes that the eliminated genes changed because they were inherently variable; however, we did not directly prove this. We also chose to use stringent selection criteria to identify a list of analyzable genes (a complete list of the data may be obtained at http://genome-www.stanford.edu/microarray) (52). We first selected only the genes that did not vary by >1.4-fold in the control comparisons. We then selected only genes having a >2-fold change in at least two of the three (RRV versus mock) hybridizations (Table 1). Hence, all of the 579 identified genes changed their level of transcriptional expression by ≥2-fold in at least two of the three RRV versus mock hybridizations and did not change their expression level by >1.4-fold in any of the control hybridizations. It is important to add that the majority of the genes (84%) which changed >2-fold in two (RRV versus mock) hybridizations also changed similarly in the third hybridization, although in some cases only by a >1.6-fold criteria (Fig. 3). Only 3 of the 579 identified genes gave divergent results in the analysis (i.e., upregulated in one array and downregulated in another) which was <0.034% of the analyzed population.

Regarding the 448 nonhuman genes (yeast and bacterial genes) spotted in the arrays as negative controls, only one passed the filter criteria in >50% of all of the hybridizations, further demonstrating the specificity of the hybridization.

Although general interpretation of microarray analysis frequently assumes that the detection and quantification of thousands of transcripts directly reflects actual changes in gene expression level, one should remember that the regulation of cellular mRNA decay rates is also an important control point in determining transcript abundance and gene expression.

A substantial difference in the number of regulated genes was observed when comparing the response at 1 and 16 hpi (Fig. 2, 3, and 5). A time course experiment was carried out to determine when during the infection the observed transcriptional responses occurred. Although the time course experi-

TABLE 3. List of transcriptionally regulated genes in Caco-2 cells after 16 h of RRV infection

| Function and gene name[a] | SwissProt accession no.[b] | FC[c] |
|---|---|---|
| **Protein modification and degradation** | | |
| *Itchy E3 ubiquitin protein ligase | P46934 | 2.6 |
| Ubiquitin ligase SMURF2 | P39940 | 2.2 |
| *Yeast homolog ubiquitin ligase Rsp5 | P46935 | 3.5 |
| Proteasome 26S subunit ATPase 3 | P17980 | 2 |
| *Matrix metalloproteinase 14 | P50281 | 3.3 |
| Disintegrin and metalloproteinase domain 9 | Q61072 | 2.1 |
| *hnRNP methyltransferase 1-like 2 | Q99873 | 2.4 |
| Cathepsin D (lysosomal aspartyl protease) | P07339 | 8.8 |
| *Lectin-like oxidized-LDL receptor 1 | P78380 | 3.8 |
| *Kallikrein 6 | Q92876 | 2.3 |
| *Ariadne (*Drosophila*) homolog | P36113 | 2.4 |
| *Ubc6p homolog | P51965 | 2.5 |
| Transmembrane protease, serine 2 | O15393 | 0.5 |
| **Transcriptional regulators** | | |
| *Transcription factor Dp-2 | Q14188 | 2.5 |
| *FOS | P01100 | 6.6 |
| *Fos-like antigen 1 | P15407 | 15 |
| *JUN | P05412 | 17 |
| *Activating transcription factor 4 | P18848 | 2.7 |
| NFκB1 | P19838 | 2.4 |
| *NFκB1E | O00221 | 5.4 |
| *E74-like factor 3 | P78545 | 3.8 |
| Thyroid hormone receptor interactor 8 | Q15652 | 2.6 |
| Far upstream element binding protein 1 | P57722 | 2.3 |
| Bromodomain adjacent to zinc-finger domain 1A | Q9UIG1 | 2.4 |
| *MAIL | Q9BYH8 | 6.4 |
| *Cyclic AMP-responsive element modulator | Q03060 | 5.4 |
| *Core promoter element binding | Q99612 | 4.3 |
| Zinc finger protein (LOC51042) (IMAGE: 471200) | | 2.8 |
| *TGFB-inducible early growth response | Q13118 | 2.9 |
| *RNA polymerase II elongation factor ELL2 | O00472 | 2.9 |
| La ribonucleoprotein | P05455 | 2.4 |
| Zinc finger protein 9 | P20694 | 2.1 |
| Zinc finger protein 216 | O76080 | 2.3 |
| Zinc finger protein 313 | ZNF313 | 2.6 |
| *DNA damage-inducible transcript 3 | P35638 | 2.5 |
| Nuclear receptor coactivator 2 | P41738 | 0.4 |
| *Transcriptional intermediary factor 1 | Q64127 | 0.4 |
| Zinc fingers and homeoboxes 1 | Q9UKY1 | 0.3 |
| *p300/CBP-associated factor | P13941 | 0.3 |
| *MAX-interacting protein 1 | P50539 | 0.4 |
| *Nuclear receptor subfamily 2, group F, member 2 | P24468 | 0.3 |
| **Apoptosis** | | |
| Programmed cell death 5 | P56812 | 2.8 |
| Apoptosis antagonizing transcription factor | Q9UNX5 | 2.2 |
| *Cytochrome *c* | P00009 | 2.6 |
| *TNF-α-induced protein 3 | P21580 | 6.5 |
| *Immediate-early response 3 | P46695 | 3.8 |
| *Baculoviral IAP repeat-containing 3 | Q13490 | 3.8 |
| *Insulin-like growth factor receptor | P08069 | 3.1 |
| SERPINB2 | P05120 | 5.7 |
| *SH3GLB2 | Q99961 | 0.5 |
| **Translation machinery** | | |
| EIF1A | Q60872 | 2.4 |
| EIF2S2 | P20042 | 2.3 |
| EIF2B2 | P49770 | 2.4 |
| EIF3S1 | O75822 | 2.5 |
| EIF3S5 | O00303 | 2.3 |
| *EIF4A1 | P04765 | 2.6 |
| SUI1 | Q9UNQ9 | 2.4 |
| Alanine-tRNA synthetase | P49588 | 2.2 |
| Lysyl-tRNA synthetase | Q15046 | 2.1 |
| Phenylalanyl-tRNA synthetase β | Q9NSD9 | 2.3 |
| Tyrosyl-tRNA synthetase | P54577 | 2.1 |
| *RNA helicase | P40562 | 4.4 |
| DEAD/H box polypeptide 3 | O00571 | 2.3 |
| *DEAD/H box polypeptide 16 | O60231 | 2.4 |
| DEAD/H box polypeptide 21 | Q64060 | 2.3 |
| DEAD/H box polypeptide Y chromosome | O15523 | 2.2 |
| *hqp0256 protein | P38712 | 2.5 |
| *Nucleophosmin 1 | P06748 | 2.6 |
| Signal recognition particle, 19 kDa | P09132 | 2.2 |
| **Cytoskeleton and cell structure** | | |
| *Actin alpha cardiac muscle | P04270 | 3.9 |
| *Actin alpha-2 smooth muscle, aorta | P03996 | 3.3 |
| Actinin alpha-4 | P08640 | 2.3 |
| Actin related protein 2/3 complex subunit 2 | O15144 | 2.1 |
| Calponin 3 acidic isoform | Q15417 | 2.6 |
| Caldesmon 1 | Q05682 | 2.9 |
| Ectodermal-neural cortex | O14682 | 2.2 |
| Thymosin beta-4 Y chromosome | O14604 | 3.1 |
| *Lymphocyte cytosolic protein 1 | P13796 | 3.3 |
| *Vimentin | P08670 | 2.1 |
| *Keratin 4 | P19013 | 3 |
| *Keratin 5 | P13647 | 3.6 |
| Keratin 15 | P19012 | 2.4 |
| *Syndecan binding protein | O17583 | 2.9 |
| Myosin light polypeptide 1 | P05976 | 2.2 |
| Tropomyosin 4 | P07226 | 2.6 |
| Bystin-like | Q13895 | 2.5 |
| *Small prolin-rich protein 1B | P22528 | 7.1 |
| *Testin | O35115 | 2.9 |
| Epithelial protein lost in neoplasma β | Q9UHB6 | 2.6 |
| *ras* homolog gene family member E | P52199 | 2.1 |
| Rho GDP dissociation inhibitor (GDI) β | P52566 | 2.7 |
| Rap1b member of RAS oncogene family | P09526 | 2.1 |
| Protein regulator of cytokinesis 1 | O43663 | 2.2 |
| *Microtubule associated protein member 1 | P40013 | 2.6 |
| **Cell adhesion and intercellular junctions** | | |
| *Cadherin 5 type 2, VE-cadherin | P33151 | 3.4 |
| Protocadherin 18 | Q9HCL0 | 2.6 |
| *CEA1 | P13688 | 3.4 |
| *CEA5 | P06731 | 2.2 |
| Catenin alpha-like 1 | Q61301 | 2.4 |
| Vinculin | P18206 | 2.5 |
| *Epithelial V-like antigen 1 | O60487 | 3.4 |
| Vascular cell adhesion molecule 1 | P19320 | 2.2 |
| *Thrombospondin 1 | P07996 | 3.9 |
| Cartilage linking protein 1 | P10915 | 2.3 |
| Occluding | Q16625 | 2 |
| *Catenin delta 1 | O60716 | 0.4 |
| **Cell cycle** | | |
| Cyclin C | P24863 | 2 |
| *Cyclin D1 | P24385 | 2.9 |
| Cyclin E1 | P24864 | 2.1 |
| *Cyclin L ania-6a | Q9UK58 | 5.1 |
| *Cyclin-dependent kinase 7 | P50613 | 2.4 |
| Pescadillo homolog 1 | P54258 | 2.1 |
| *BTG family member 2 | P78543 | 2.5 |
| *Cyclin G2 | Q16589 | 0.3 |
| Cyclin-dependent kinase inhibitor 1B | P46527 | 0.5 |
| *Putative lymphocyte $G_0/G_1$ switch gene | P27469 | 0.2 |
| Damage-specific DNA binding protein 1 | Q16531 | 0.4 |
| *Ataxia telangiectasia mutated | P42346 | 0.4 |
| **Cellular development and differentiation** | | |
| *Retinoic acid induced 3 | O95357 | 5.1 |
| *Fibroblast growth factor 7 | P21781 | 2.7 |
| *Enhancer filamentation 1 | Q14511 | 2.3 |
| Oncogene TC21 | P10833 | 2.2 |
| *N-myc downstream regulated | Q92597 | 3 |
| *Ras association (RalGDS/AF-6) domain family 1 | O60539 | 2.2 |
| *Tax interaction protein 1 | O14907 | 2.8 |
| *Nucleolar protein p40 | Q99848 | 3 |
| *Epithelial membrane protein 1 | P54849 | 4.2 |
| **RNA processing and modification** | | |
| *U3 snoRNP-associated 55-kDa protein | O43818 | 2.4 |
| *Nucleolar protein 1,120 kDa | P46087 | 2.7 |
| Splicing factor arginine/serine-rich 7 | Q16629 | 2.2 |
| Splicing factor arginine/serine-rich 3 | P23152 | 2.3 |
| *Heterogeneous ribonucleoprotein A/B | Q99383 | 2.3 |
| Heterogeneous ribonucleoprotein C | P07910 | 2.7 |
| *Phorbolin | Q9UH17 | 2.8 |
| **Kinases and phosphatases** | | |
| NF-kappa-β-induced kinase | Q99558 | 2.4 |
| PCTAIRE protein kinase 2 | Q00537 | 2 |
| *Serum-inducible kinase | Q9NYY3 | 3.2 |
| Serum/glucocorticoid regulated kinase | O00141 | 2.5 |
| Protein tyrosine kinase 2β | Q14289 | 2.5 |
| Kinase insert domain receptor | P35968 | 2.7 |
| Uridine monophosphate kinase | P52623 | 2.3 |
| Hexokinase 2 | P52789 | 2.6 |
| Ethanolamine kinase (EKI1) | Q9HBU6 | 2.2 |
| Tyrosine 3-monooxygenase | P29312 | 2.5 |
| *Cyclic AMP-dependent protein kinase inhibitor β | P27775 | 2.5 |
| Protein phosphatase 2A, β-isoform | P11082 | 2 |
| *MKP-1 like protein tyrosine phosphatase | P28563 | 2.8 |
| *Dual specificity phosphatase 6 | Q16828 | 2.6 |
| Pyrophosphatase inorganic | Q15181 | 2.3 |
| *MINPP1 (IMAGE: 592630) | | 0.4 |
| **Lipid biosynthesis and drug metabolism** | | |
| *Dual adaptor of phosphotyrosine | Q9UN19 | 5.8 |
| *Phospholipid scramblase 1 | P47140 | 2.5 |
| *Niemann-Pick disease type C1 | O15118 | 2.4 |
| Stomatin-like 1 | Q9UBI4 | 2.1 |
| *Cytochrome $b_5$ reductase b5R.2 | P20070 | 3.6 |
| *Fatty acid coenzyme A ligase long-chain 4 | O60488 | 2.7 |
| *Alpha-methylacyl-coenzyme A racemase | P70473 | 0.5 |
| *CTP synthase | P17812 | 3.3 |
| Cytochrome $P_{450}$ subfamily IIB polypeptide 6 | P20813 | 2.3 |
| **Stress response** | | |
| *HspC030 | Q9Y6D0 | 2.4 |
| *Hsp40 | Q9QYJ3 | 7.2 |
| *Hsp70 protein-like 1 | P34931 | 6.7 |
| *Tumor rejection antigen 1 | P14625 | 2.7 |
| *GrpE-like protein cochaperone | P97576 | 2.5 |
| *Sperm-associated antigen 1 | P50503 | 2.6 |
| *Crystalline alpha B | O43416 | 4.3 |
| *Small stress protein-like protein Hsp22 | Q9UJY1 | 4.7 |
| *Chaperonin containing TCP1 subunit 5ε | P48643 | 2.8 |
| Chaperonin containing TCP1 subunit 4δ | P50991 | 2.3 |
| *Chaperonin containing TCP1 subunit 6A (zeta 1) | P40227 | 2.2 |
| Peptidylprolyl isomerase B | P23284 | 2.2 |
| Oxidative-stress responsive 1 | Q9Z1W9 | 2.3 |
| Clusterin | P10909 | 2.2 |
| Heat shock 70-kDa protein 1B | P08107 | 0.4 |
| **IFN response** | | |
| *IFN-related developmental regulator 1 | O00458 | 6.3 |
| *IFN-regulatory factor 2 | P14316 | 2.6 |
| *2′-5′-oligo(A) synthetase 1 (OAS1) | P00973 | 5 |
| IFN induced with tetraticopeptide repeats 1 | P09914 | 3.8 |
| IFN-γ-inducible protein 16 | Q16666 | 2.7 |
| *Guanylate binding protein 1, 67 kDa | P32455 | 6.2 |
| **Immune response** | | |
| Small inducible cytokine A5 (RANTES) | P13501 | 2.6 |
| *IL-2 receptor beta | P14784 | 2.9 |
| *IL-1 receptor accessory protein | Q02955 | 2.4 |
| *UL16 binding protein 2 | Q9BZM5 | 3.5 |
| Pregnancy-specific β-1-glycoprotein 1 | P11464 | 3 |
| Chornichon-like | O95406 | 2.1 |
| *Prostaglandin-endoperoxide synthase 2 | P35354 | 3.5 |
| *Leukotriene A4 hydrolase | P09960 | 2.7 |
| *Spermine synthase | P52788 | 3.4 |
| *Spermidine/spermine *N1*-acetyltransferase | P21673 | 6.7 |
| **S*-Adenosylmethionine decarboxylase 1 | P17707 | 2.6 |
| *Amiloride-binding protein 1 | P19801 | 0.4 |
| **Membrane transporters** | | |
| $K^+$ channel subfamily K member 1 | O00180 | 2.2 |
| *Zinc/iron regulated transporter-like | Q9BTV0 | 2.4 |
| *ATP-binding cassette subfamily G member 2 | Q9UNQ0 | 2.9 |
| Solute carrier family 2 member 3 | P11169 | 2.5 |
| Solute carrier family 26 member 3 | P40879 | 2.2 |
| Kynurenine 3-monooxygenase | Q9H1Y5 | 2 |
| Transferrin receptor | P02786 | 2.3 |
| Ferredoxin 1 | P10109 | 2.1 |
| *Thioredoxin reductase 1 | Q16881 | 2.5 |
| *IMP dehydrogenase 2 | P12268 | 2.3 |
| *Steroid-5-alpha reductase, alpha polypeptide 1 | P18405 | 6.4 |
| *Methylene tetrahydrofolate dehydrogenase 2 | P36776 | 2.8 |
| *$K^+$ voltage-gated channel subfamily H member3 | Q12809 | 0.4 |
| *Solute carrier family 11 member 3 | Q9NRL0 | 0.3 |
| *Duodenal cytochrome *b* | P49447 | 0.3 |
| **Signal transduction** | | |
| *Integrin-$\alpha_6$ | P23229 | 2.7 |
| *Plasminogen activator urokinase receptor | Q03405 | 4.7 |
| Tetraspan NET-7 | O95858 | 2.7 |
| Zinc finger protein 259 | O75312 | 2.3 |
| SBBI31 protein (IMAGE: 429470) | | 2.3 |
| *TNF receptor superfamily member 11b | P20333 | 4.4 |
| *Oncogene ERBB3 | P21860 | 0.4 |
| Vav 3 oncogene | Q9UKW4 | 0.4 |
| *Ral guanine nucleotide exchange factor | Q9NZ16 | 0.4 |
| Epidermal growth factor receptor | P00533 | 0.5 |
| **Vesicle formation and intracellular transport** | | |
| *Caveolin 1 | Q03135 | 3 |
| *Caveolin 2 | P51636 | 3.6 |
| *PI-clathrin assembly protein | Q13492 | 2.6 |

*Continued on following page*

TABLE 3—*Continued*

| Function and gene name[a] | SwissProt accession no.[b] | FC[c] |
|---|---|---|
| Adaptor-related protein complex 3, β2 subunit | P21851 | 2.2 |
| *ADP-ribosylation factor binding protein GGA3 | P22892 | 2.2 |
| Myosin X | P19524 | 2 |
| *RAB31, RAS oncogene family | Q13636 | 2.7 |
| Syntaxin 3A | Q13277 | 2.5 |
| *Myomegalin | P25386 | 0.4 |
| CNS-specific functions and neuropeptides | | |
| *Neuronal protein (NP25) | Q9UI15 | 6.3 |
| *SRY-box 11 (SOX11) | P35716 | 6.4 |
| *Dunce-like phosphodiesterase E4 | Q07343 | 3.4 |
| *Gamma-aminobutyric acid A receptor γ2 | P18507 | 2.8 |
| Huntington-associated protein interacting protein | O60229 | 2.2 |
| *Cholecystokinin | P06307 | 4.4 |
| *Glycoprotein hormones α polypeptide | P01215 | 14.7 |
| *Gamma-aminobutyric acid A receptor ε | P78334 | 0.4 |
| Enzymes | | |
| *N*-Acetylneuraminic acid phosphatase synthase | Q12999 | 2.3 |
| Iduronidase alpha L | P35475 | 2.1 |
| *Rab geranylgeranyltransferase, β subunit | P53611 | 2.7 |
| Phosphorylase, glycogen; liver | P06737 | 2.1 |
| Enolase 1, alpha | P06733 | 2.2 |
| *Glutathione *S*-transferase A2 | P09210 | 2.6 |
| *Glutathione *S*-transferase A3 | Q16772 | 2.8 |
| Leucine aminopeptidase | P28838 | 2.4 |
| *Putative *b,b*-carotene-9′,10′-dioxygenase | Q03393 | 2.9 |
| *Solute carrier family 3, member 2 | P40884 | 2.2 |
| *Indolethylamine *N*-methyltransferase | O95050 | 3.1 |
| Aminopeptidase A | Q07075 | 2.2 |
| UDP-glucose ceramide glucosyltransferase | Q16739 | 2.3 |
| Alpha-2,3-sialyltransferase | Q02734 | 0.5 |
| *Mannosidase alpha class 1A, member 1 | P33908 | 0.3 |
| Glycogen debranching enzyme | P35573 | 0.4 |
| PFKFB4 | Q16877 | 0.5 |
| Sorbitol dehydrogenase | Q00796 | 0.4 |
| Viral receptors | | |
| *Decay accelerating factor for complement | P08174 | 2.7 |
| Integrin $\alpha_2$ | P17301 | 3.1 |
| Integrin $\beta_1$ | P05556 | 2.8 |
| Calcium homeostasis | | |
| *S100 calcium-binding protein A8 | P05109 | 4.6 |
| S100 calcium-binding protein A3 (S100A3/S110E) | P33764 | 3.1 |
| Reticulocalbin 1, EF-hand calcium binding domain | Q15293 | 2.5 |
| $Ca^{2-}$ channel voltage-dependent, L type subunit α1D | Q01668 | 2.1 |
| *Annexin A9 | Q07936 | 0.4 |
| *Stanniocalcin 1 | P52823 | 0.4 |
| Histones | | |
| H1 histone family member 2 | P16403 | 2.2 |
| *H2A histone family member N | P02262 | 2.1 |
| Miscellaneous | | |
| WD repeat domain 1 | O88342 | 2.6 |
| *Transmembrane 4 superfamily member 1 | P30408 | 3.5 |
| *Nucleolar phosphoprotein Nopp34 | Q9BYG3 | 2.6 |
| Sperm-associated antigen 9 | P34609 | 2.5 |
| Albumin | P02768 | 3.8 |
| Prion protein (p27-30) | P04156 | 2.4 |
| Reticulon 2 (RTN2/NSP2/NSPL1) | O75298 | 2.4 |
| *Cysteine- and hystidine-rich domain (CHORDC1) | Q9NZ93 | 2.8 |
| Semaphorin L | O75326 | 2.4 |
| *Dedicator of cytokinesis 3 (IMAGE: 39922) | | 2.3 |
| *Schwannomin-interacting protein 1 (IMAGE: 506143) | | 3.6 |
| Uncharacterized bone marrow protein BM040 | Q9NZ82 | 2.2 |
| *Enhancer of polycomb 1 | Q9H7T7 | 2.6 |
| Human proteinase activated receptor-2 mRNA, 3′ UTR | P39195 | 2.2 |
| *Arginine-rich, mutated in early-stage tumors | Q9N3B0 | 3.1 |
| *Epithelial stromal interaction 1 (IMAGE: 1855351) | | 2.3 |
| *PVT1 (murine) oncogene homolog (IMAGE: 295410) | | 2.8 |
| *GE36 gene | Q9H2B6 | 2.5 |
| *Desmoplakin | P15924 | 3 |
| *Laminin, gamma 2 | Q13753 | 3.6 |
| *Cylindromatosis (turnban tumor syndrome) | Q9NQC7 | 3.1 |
| *Serine (or cysteine) proteinase inhibitor | P05120 | 5.7 |
| *Brain-specific protein | Q9Y326 | 4.6 |
| Cornichon-like | O95406 | 2.1 |
| Karyopherin alpha 2 | P52292 | 2.2 |
| Phorbolin like protein MDS019 | Q9UH17 | 3.1 |
| Hematological and neurological expressed 1 | Q9UK76 | 2.3 |
| Reelin | P78509 | 3.5 |
| *Golgin 67 | Q9NZW0 | 0.5 |
| Synaptogyrin 1 (SYNGR1) | O43759 | 0.5 |
| *Semaphorin 4G | Q9WUH7 | 0.2 |
| *Disabled (*Drosophila*) homolog 1 | O75553 | 0.4 |
| **H. sapiens* LUCA-15 protein mRNA | P52756 | 0.3 |
| *G protein-coupled receptor GPRC5B | Q9NZH0 | 0.3 |
| *Upregulated by 1,25-dihydroxyvitamin $D_3$ | Q9H3M7 | 0.3 |
| Wilm's tumor 1-associating protein | Q15007 | 0.4 |
| HP1-BP74 | Q9UHY0 | 0.4 |
| TACC2 | O95359 | 0.4 |
| Mitochondrial ribosomal protein S14 | O60783 | 0.4 |
| Sorting nexin 17 | Q15036 | 0.5 |
| Lipin 2 | Q92539 | 0.5 |
| Amyotrophic lateral sclerosis 2 | Q9C0K7 | 0.4 |
| *Pleckstrin homology domain interacting protein | Q9H261 | 0.3 |
| Human reported sequences[d] | | |
| *IMAGE: 1619049 COBW-like protein | | 2.6 |
| *IMAGE: 70578 hypothetical protein FLJI1362 | | 3.1 |
| *IMAGE: 858375 cDNA DKFZp566J1846 | | 2.6 |
| *IMAGE: 788213 | | 2.5 |
| *IMAGE: 32241 KIAA0410 gene product | | 2.6 |
| *IMAGE: 1659910 | | 2.5 |
| *IMAGE: 824031 | | 2.4 |
| *IMAGE: 841207 euroimage 2005735 | | 2.9 |
| *IMAGE: 814117 | | 2.5 |
| *IMAGE: 753907 cDNA DKFZp434G227 | | 3.5 |
| *IMAGE: 1569107 hypothetical protein FLJ20624 | | 3 |
| *IMAGE: 1947865 ORF | | 2.5 |
| *IMAGE: 731270 hypothetical protein FLJ20093 | | 2.6 |
| *IMAGE: 782195 DNA from clone RP13-329D4 | | 2.2 |
| *IMAGE: 1619219 | | 2.7 |
| *IMAGE: 843250 EST | | 2.2 |
| *IMAGE: 700625 CGI-09 protein | | 2.6 |
| *IMAGE: 531343 KIAA0005 gene product | | 2.9 |
| *IMAGE: 711993 KIAA1382 | | 2.2 |
| *IMAGE: 743190 | | 2.4 |
| *IMAGE: 1553025 hypothetical protein FLJ20291 | | 3.3 |
| *IMAGE: 470232 | | 3 |
| *IMAGE: 502396 chromosome 21 ORF50 | | 4.3 |
| *IMAGE: 1657336 FLJ13672 fis clone PLACE1011749 | | 2.9 |
| *IMAGE: 130747 FLJ13522 fis clone PLACE1005884 | | 2.9 |
| *IMAGE: 61626 Putative 28-kDa protein | | 3.0 |
| *IMAGE: 796508 KIAA0690 protein | | 3.5 |
| *IMAGE: 447520 FLJ14241 fis clone OVARC1000533 | | 11. |
| *IMAGE: 461365 | | 3.7 |
| *IMAGE: 666138 DKFZp761J1523 protein | | 4.1 |
| *IMAGE: 1929737 | | 2.5 |
| *IMAGE: 1689557 euroimage 1034327 | | 2.9 |
| *IMAGE: 290399 DKFZp5661133 protein | | 2.6 |
| *IMAGE: 712604 | | 2.2 |
| *IMAGE: 289496 EST | | 4.8 |
| *IMAGE: 235909 FLJ22554 fis clone HSI01092 | | 2.5 |
| *IMAGE: 1536727 hypothetical protein MGC11324 | | 2.2 |
| *IMAGE: 1628121 | | 3.4 |
| *IMAGE: 23933 clone 23933 mRNA sequence | | 2.5 |
| *IMAGE: 773324 hypothetical protein FLJ10439 | | 2.4 |
| *IMAGE: 1031402 hypothetical protein | | 2.7 |
| *IMAGE: 1625869 hypothetical protein F23149_1 | | 2.2 |
| IMAGE: 54601 | | 2.3 |
| *IMAGE: 809533 hypothetical protein MGC14376 | | 3.8 |
| *IMAGE: 489729 FLJ10768 fis clone NT2RP4000150 | | 5.3 |
| *IMAGE: 79632 hypothetical protein MGC13007 | | 2.3 |
| *IMAGE: 263342 hypothetical protein | | 2.4 |
| *IMAGE: 1638584 | | 3.4 |
| *IMAGE: 283723 hypothetical protein FLJ11021 | | 2.9 |
| *IMAGE: 950894 DKFZp761C169 protein | | 2.3 |
| *IMAGE: 531036 hypothetical protein MGC2975 | | 4.3 |
| *IMAGE: 130243 hypothetical protein FLJ11036 | | 4.7 |
| *IMAGE: 45912 euroimage 45912 | | 2.5 |
| *IMAGE: 415976 FLJ13903 fis clone THYRO1001854 | | 3.1 |
| IMAGE: 1565576 | | 3 |
| IMAGE: 788507 | | 2.3 |
| IMAGE: 809733 | | 2.3 |
| IMAGE: 826130 KIAA1527 protein | | 2 |
| IMAGE: 328889 | | 2.3 |
| IMAGE: 1619109 | | 2.4 |
| IMAGE: 1740325 | | 2.1 |
| IMAGE: 825271 KIAA0029 protein | | 2.1 |
| IMAGE: 767163 hypothetical protein FLJ20425 | | 2.7 |
| IMAGE: 80463 | | 2.3 |
| IMAGE: 1606603 | | 2.1 |
| IMAGE: 1891596 | | 2.6 |
| IMAGE: 1032444 clone IMAGE: 3354845 | | 2.2 |
| IMAGE: 111437 | | 2.6 |
| IMAGE: 305843 CGI-47 protein | | 2.1 |
| IMAGE: 784168 DKFZp564A072 | | 2.3 |
| IMAGE: 77361 CGI-97 protein | | 2.6 |
| IMAGE: 302997 hypothetical protein FLJ20036 | | 2.6 |
| IMAGE: 261472 putative nuclear protein ORF1FL49 | | 3.1 |
| IMAGE: 449329 | | 2.2 |
| IMAGE: 814988 FLJ23130 fis clone LNG08419 | | 2.4 |
| IMAGE: 49879 DKFZp761H229 | | 2.4 |
| IMAGE: 1696061 | | 2.6 |
| IMAGE: 713031 clone, IMAGE: 3457003 | | 2.4 |
| IMAGE: 489106 hypothetical protein FLJ11210 | | 2.5 |
| IMAGE: 1836586 | | 2.6 |
| IMAGE: 563860 | | 2.4 |
| IMAGE: 75044 | | 2.6 |
| IMAGE: 757265 hypothetical protein MGC4399 | | 2.7 |
| IMAGE: 812069 DKFZp586F1323 | | 2.2 |
| IMAGE: 884346 hypothetical protein FLJ20323 | | 2.4 |
| IMAGE: 666110 KIAA0580 protein | | 2.1 |
| IMAGE: 357117 hypothetical protein FLJ13194 | | 2.2 |
| IMAGE: 1713773 | | 2.2 |
| IMAGE: 251769 | | 2.1 |
| IMAGE: 52128 | | 2.1 |
| IMAGE: 491465 DKFZp4340531 protein | | 2.3 |
| IMAGE: 1524481 | | 2.2 |
| IMAGE: 454970 DKFZp434G032 protein | | 3.2 |
| IMAGE: 529302 FLJ11765 fis clone HEMBA 1005891 | | 2.1 |
| IMAGE: 588492 | | 3 |
| IMAGE: 713205 CGI-94 protein | | 2.4 |
| IMAGE: 502201 | | 2.2 |
| IMAGE: 1856516 | | 2.1 |
| IMAGE: 1950727 | | 2.2 |
| IMAGE: 629498 | | 2.2 |
| IMAGE: 1696757 hypothetical protein KIAA1165 | | 2.3 |
| IMAGE: 502739 hypothetical protein FLJ11010 | | 2.1 |
| IMAGE: 265626 | | 2.3 |
| IMAGE: 358333 FLJ20153 fis clone COL08656 | | 2.3 |
| IMAGE: 429446 | | 2.5 |
| IMAGE: 428529 | | 2.4 |
| IMAGE: 1536628 | | 2.4 |
| IMAGE: 771165 hypothetical protein FLJ14697 | | 2.2 |
| IMAGE: 1570339 clone, IMAGE: 3948909 | | 2.3 |
| IMAGE: 452863 hypothetical protein AD034 | | 2.2 |
| IMAGE: 449403 | | 2.7 |
| IMAGE: 45801 | | 2.4 |
| IMAGE: 428824 hypothetical protein FLJ13605 | | 2.7 |

*Continued on following page*

TABLE 3—*Continued*

| Function and gene name[a] | SwissProt accession no.[b] | FC[c] | Function and gene name[a] | SwissProt accession no.[b] | FC[c] | Function and gene name[a] | SwissProt accession no.[b] | FC[c] |
|---|---|---|---|---|---|---|---|---|
| IMAGE: 840467 hypothetical protein FLJ11259 | | 2.5 | *IMAGE: 588368 KIAA0947 protein | | 0.4 | IMAGE: 950945 cDNA DKFZp564P0823 | | 0.4 |
| IMAGE: 488155 hypothetical protein FLJ12787 | | 2.7 | *IMAGE: 461118 EST | | 0.4 | IMAGE: 725143 hypothetical protein FLJ22418 | | 0.4 |
| *IMAGE: 45601 EST | | 2.3 | *IMAGE: 1909433 DKFZp727C091 protein | | 0.4 | IMAGE: 502794 FLJ21435 fis clone COL04244 | | 0.4 |
| IMAGE: 1916461 hypothetical protein | | 2.6 | *IMAGE: 826622 KIAA0430 gene product | | 0.4 | IMAGE: 111006 | | 0.4 |
| IMAGE: 811572 | | 2.4 | *IMAGE: 1909873 FLJ20051 protein | | 0.4 | IMAGE: 742569 hypothetical protein FLJ00026 | | 0.4 |
| IMAGE: 773331 clone RP11-353C18 | | 2.4 | *IMAGE: 80292 FLB3344 PRO0845 | | 0.4 | IMAGE: 412989 FLJ13634 fis PLACE1011133 | | 0.4 |
| *IMAGE: 815069 cDNA DKFZp564D0472 | | 0.4 | *IMAGE: 22908 EST | | 0.3 | IMAGE: 29965 FLJ22071 fis clone HEP11691 | | 0.4 |
| *IMAGE: 1570502 FLJ12936 fis NT2RP200518 | | 0.4 | *IMAGE: 840974 hypothetical protein FLJ10743 | | 0.5 | IMAGE: 298937 hypothetical protein dJ551D2.5 | | 0.4 |
| *IMAGE: 40120 KIAA0941 protein | | 0.4 | *IMAGE: 1552117 EST | | 0.4 | IMAGE: 624379 KIAA0740 gene product | | 0.4 |
| *IMAGE: 131099 FLJ13057 protein | | 0.3 | *IMAGE: 126851 hypothetical protein FLJ11160 | | 0.5 | IMAGE: 296616 hypothetical protein FLJ21174 | | 0.5 |
| *IMAGE: 841146 DKFZp566G1424 protein | | 0.3 | *IMAGE: 291426 KIAA1846 protein | | 0.4 | IMAGE: 259953 KIAA1600 protein | | 0.4 |
| *IMAGE: 1836834 KIAA1055 protein | | 0.4 | *IMAGE: 256947 EST | | 0.3 | IMAGE: 47080 hypothetical protein MGC13033 | | 0.5 |
| *IMAGE: 285312 | | 0.4 | *IMAGE: 32206 KIAA0774 protein | | 0.3 | IMAGE: 1853547 KIAA1572 protein | | 0.5 |
| *IMAGE: 32805 | | 0.3 | *IMAGE: 767172 euroimage 248114 | | 0.4 | IMAGE: 811025 hypothetical protein | | 0.4 |
| *IMAGE: 240896 hypothetical protein | | 0.4 | *IMAGE: 238907 protein, Strait02270_FL142 | | 0.4 | IMAGE: 303139 hypothetical protein FLJ14054 | | 0.4 |
| *IMAGE: 342399 cDNA DKFZp434A2410 | | 0.4 | *IMAGE: 135106 DKFZp434C0328 | | 0.4 | IMAGE: 742596 | | 0.4 |
| *IMAGE: 824312 FLJ10229 fis HEMBB1000136 | | 0.4 | *IMAGE: 1461528 EST | | 0.3 | IMAGE: 665127 clone 747H23 chrom 6q13-15 | | 0.5 |
| *IMAGE: 69378 FLJ23165 fis clone LNG09846 | | 0.5 | IMAGE: 26414 | | 0.4 | IMAGE: 435208 | | 0.5 |
| *IMAGE: 951068 cDNA DKFZp566E183 | | 0.4 | *IMAGE: 814616 EST | | 0.4 | IMAGE: 1160531 | | 0.5 |
| *IMAGE: 32495 FLJ22150 fis clone HRC00109 | | 0.5 | *IMAGE: 428782 hypothetical protein PRO2730 | | 0.3 | IMAGE: 1883621 | | 0.4 |
| *IMAGE: 427797 | | 0.4 | *IMAGE: 1908712 hypothetical protein | | 0.4 | IMAGE: 1622129 | | 0.4 |
| *IMAGE: 429433 MGC11242 protein | | 0.3 | *IMAGE: 196435 EST | | 0.4 | IMAGE: 45921 human clone 23908 mRNA | | 0.5 |
| *IMAGE: 767721 FLJ13604 fis PLACE1010401 | | 0.3 | *IMAGE: 46896 hypothetical protein PRO1331 | | 0.3 | IMAGE: 247216 DKFZp586F1322 | | 0.5 |
| *IMAGE: 1926272 EST | | 0.4 | IMAGE: 784258 hypothetical protein my014 | | 0.5 | IMAGE: 1900362 | | 0.4 |
| *IMAGE: 212542 FLJ12900 fis NT2RP2004321 | | 0.5 | IMAGE: 773185 | | 0.4 | IMAGE: 71730 FLJ21278 fis clone COL01832 | | 0.4 |
| *IMAGE: 132015 hypothetical protein FLJ23516 | | 0.4 | IMAGE: 51879 | | 0.4 | IMAGE: 725473 DNA segment on chromosome | | 0.5 |
| *IMAGE: 429811 *Homo sapiens* clone 122482 | | 0.3 | IMAGE: 451646 KIAA0924 | | 0.4 | IMAGE: 646753 | | 0.4 |
| *IMAGE: 1055460 | | 0.4 | IMAGE: 1656557 | | 0.4 | IMAGE: 1627504 | | 0.4 |
| *IMAGE: 42935 EST | | 0.4 | IMAGE: 503671 FLJ14368 fis HEMBA 1001122 | | 0.3 | | | |
| | | | IMAGE: 1049346 hypothetical protein | | 0.4 | | | |
| | | | IMAGE: 511091 | | 0.4 | | | |
| | | | IMAGE: 194399 cDNA DKFZp586B1722 | | 0.22 | | | |

[a] As registered in SMD (52). Some genes are grouped according to related biological function. *, Genes whose transcriptional level changed more than twofold in all three experimental hybridizations (see Table 1).

[b] Not indicated for human reported sequences. For genes that do not have a SwissProt accession number, the IMAGE number is indicated. The SwissProt entry is copyright. It is produced through a collaboration between the Swiss Institute of Bioinformatics and the EMBL outstation of the European Bioinformatics Institute. There are no restrictions on its use by nonprofit institutions as long as its content is in no way modified, and this statement is not removed. Usage by and for commercial entities requires a license agreement (see http://www.isb-sib.ch/announce/).

[c] FC, fold change. Values of >2 and <0.5 correspond to up- and downregulated genes, respectively.

[d] As reported in the IMAGE human cDNA collection (36) (also traceable at http://genome-www5.stanford.edu/cgi-bin/SMD/source/sourceSearch/).

ment did not include the extensive number of controls and duplicates used in our primary experiment, the results clearly show that very few of the transcriptional changes observed at 16 hpi are detected at 6 hpi (Fig. 5 and Table 2). Hence, it seems likely that the majority of host transcriptional changes observed are not due to the early host cell binding and entry events, although direct experiments need to be carried out to confirm this hypothesis.

At 16 hpi we detected 508 genes (represented by 576 array elements), out of 8,575 analyzable genes, that were up- or downregulated. This number represents 6.7% of the analyzable genes. Several studies of the transcriptional response to other viral infections have recently been reported (7, 20, 21, 42, 60), and a brief discussion of these studies is provided. Based on the reported numbers of regulated and total analyzed genes in previous reports, the percentage of modulated transcripts after virus infection varies between 1.3 and 7% (7, 20, 21, 60). Infection of primary human foreskin fibroblasts with human cytomegalovirus (60), and the $CD4^+$ T-cell line CEM-CCRF with HIV-1-LAI (21) produced a balanced mix between up- and downregulated genes. Similar findings were observed when human keratinocytes were transfected with HPV31 cDNA (7). In contrast, influenza virus infection of HeLa cells (20) induced a transcriptional response characterized primarily by downregulation. In all cases, as in RRV infection, the magnitude of the response increased over time. This is not surprising since, with increasing time, more stages of the virus replication cycle occur and more viral proteins are expressed. These ongoing steps in viral replication can activate additional signal transduction pathways that can generate new responses in the cell. In addition, the increase of the transcriptional responses over time could be due to paracrine effects in which newly synthesized proteins from infected cells interact with neighboring uninfected cells, resulting in additional transcriptional changes.

**Comparison with previous reports of rotavirus-induced responses.** Rotavirus infection induces profound alterations in the morphology and biochemistry of the host cell; however, the molecular mechanisms underlying these events are not fully understood. Previous work in MA104 cells demonstrated an upregulation, at the mRNA and protein level, of BiP (grp78)

and endoplasmin (grp94, tumor rejection antigen 1), two proteins resident of the ER, and members of a family of glucose-regulated chaperones (58). In accordance with that report, we also found upregulation of the gene that encodes endoplasmin (grp94, tumor rejection antigen 1); unfortunately, we could not evaluate the transcriptional response of Bip (grp78) because this gene was excluded from our analysis due to its variability in the control comparisons (mock versus mock). Supporting the hypothesis that cellular chaperones might be involved in the process of rotavirus maturation in the ER, we did find upregulation of members of the major classes of general chaperons such as HSP40, HSP70, and HSP90 that assist the folding process in the ER (see Table 3, stress response category).

Increases in cytokine gene expression in response to rotavirus infection had previously been reported by Rollo et al. (46). The transcriptional activity of genes encoding a variety of chemokines in HT-29 cells was analyzed by RT-PCR. These authors reported the induction of C-X-C chemokines, including interleukin-8 (IL-8), IP-10, and GROγ, and the induction of C-C chemokines such as RANTES and monocyte chemoattractant protein 1 (MCP1). In addition, genes encoding IFN-α and granulocyte-macrophage colony-stimulating factor (GM-CSF) were found to be upregulated in this analysis. Conversely, the transcripts for tumor necrosis factor alpha (TNF-α), IL-1α, IL-1β, and IFN-β were not increased after rotavirus infection of HT-29 cells. In agreement with these previous reports, the level of mRNA encoding RANTES was upregulated 2.6-fold in our analysis. The gene that encodes GROγ was not present on the microarrays in this study. We also found a slight upregulation of GM-CSF and GROα, but these genes were not included in our final listing because they did not reach the twofold threshold value. The transcriptional response of IL-6, MCP1, and TNF-α genes was not evaluated due to their variability in the control comparisons, and the genes encoding for IP10, IL-1α, and IL-1β were not analyzed because they were not present on the microarrays.

Examination and analysis of the list of 508 regulated genes identified several families of genes with different functions (Table 3). Some of these groups include genes encoding integral membrane proteins, IFN-related genes, transcriptional and translational regulators, and others. Some of these may be involved in processes such as viral replication or cell defense. A clear understanding of the mechanistic relationship between transcriptional regulation changes and rotavirus replication will require additional studies. However, it is reasonable to begin to examine some of the data obtained here and to speculate on possible relationships between the host transcriptional response observed and the viral replication cycle.

**Viral cellular receptors are upregulated in RRV-infected Caco-2 cells.** Among the transcripts upregulated in infected Caco-2 cells, integrin $\alpha_2$ and integrin $\beta_1$ were identified. Interestingly, it has been shown that integrin $\alpha_2\beta_1$ can mediate attachment and entry of rotavirus into cells (26). Other integrins that were also implicated in rotavirus entry did not pass the filter criteria in this analysis (integrin $\alpha_4$) (26), were not included in the array (integrin $\alpha_5$) (24), or were not upregulated on the basis of our criteria (integrin $\beta_3$) (24). The transcript of a homolog of HSP70, HSPA1L, was also upregulated in rotavirus-infected cells. Members of this family of heat shock proteins have been proposed to mediate rotavirus entry in MA104 cells (23). The mRNA transcript for sialic acid synthase, an enzyme involved in the biosynthetic pathway of sialic acids, was also upregulated. Some animal strains of rotavirus, including RRV, attach to sialic acid moieties on the cell surface prior to cell entry (18, 31). Although the protein expression of these putative viral receptor transcripts needs to be directly measured, upregulation of these receptor mRNAs raises several interesting possibilities. Rotavirus infection might upregulate expression of its own cellular receptor to facilitate viral entry. In this way the infected cell would be more likely to be suprainfected with new infectious particles, although the importance of suprainfection of cells "in vivo" is not known. Another possibility is that rotavirus infection might enhance receptor upregulation in surrounding uninfected cells, thereby facilitating the spread of the infection. Since 75% of the cells were infected in our experiments (Fig. 1) and mRNA from all of the cells in the infected flasks was examined, we cannot determine from this analysis if integrin, HSPA1L, or sialic acid synthase regulation took place in the noninfected surrounding cells. It will be interesting to carry out additional studies at lower MOIs, sort infected and noninfected cells, and then look at the cellular response in the two separate populations. It is also possible that the cell upregulated the expression of putative rotavirus receptors as a defense mechanism to block viral release and spread. Overexpression of the rotavirus receptors in infected cells could mediate binding and "neutralization" of the newly formed and shed viral particles. It has been shown that high levels of cell surface expression of CD4, the cellular receptor for HIV-1, reduces the infectivity of the released virions by sequestering the viral envelope (34).

**Translation regulation in RRV-infected Caco-2 cells.** Several genes involved in protein synthesis were upregulated after rotavirus infection. These include six eukaryotic translation initiation factors (eIF1A, eIF2S2, eIF2B2, eIF3S1, eIF3S5, and eIF4A1), four tRNA synthetases (alanyl, phenylalanyl, lysyl, and tyrosyl tRNA synthases), and four DEAD box proteins (DEAD/H box polypeptides 3, 16, and 21 and Y chromosome) (putative RNA helicases, involved in translation initiation). No translation elongation factors were found to be modulated in this analysis. It has been shown that rotavirus infection mediates a reduction of cellular protein synthesis, favoring translation of viral proteins (25, 45). If the upregulation of the translation associated genes seen here is correlated with an upregulation of the corresponding host proteins, one might speculate that rotavirus induces an upregulation of the protein translation machinery of the cell and uses this machinery for the synthesis of its own proteins, while simultaneously blocking host cellular protein synthesis. In this manner, two mechanisms could be used by the virus for efficient translation of its own proteins. One would involve an upregulation of cellular translation factors for a more efficient translation of viral proteins, and the other would direct the cell translation machinery to specifically favor viral genes due to the specific interaction of NSP-3 and eIF4G1 (45).

**IFN response to RRV infection.** Among the 508 genes differentially regulated after 16 h of rotavirus infection, six are IFN-inducible genes: 2′5′-oligoadenylate synthetase 1 (OAS1), IFN regulatory factor 2 (IRF2), IFN-related developmental regulator 1 (IFRD1), IFN-induced protein with tetratricopep-

tide repeats 1 (IFIT1), guanylate binding protein 1 (GBP1), and IFN-γ-inducible protein 16 (IFI16).

IFNs are a large family of secreted proteins that were initially discovered because of their antiviral activity. It is clear now that, in addition to this function, IFNs also modulate cell growth, immune response, and antitumor activities (reviewed in references 50 and 53). The IFN-induced gene products that play a major role in fighting viral infections include OAS1, RNase L, the Mx proteins, and the PKR protein kinase (47). Among the IFN-regulated genes that were differentially expressed in this study, we found several genes whose products have been previously shown to establish an antiviral state during viral infections, including IRF2, OAS1, and GBP1. The upregulation of the gene encoding OAS1 is potentially significant. This synthetase is stimulated by dsRNA to produce 2′-5′-linked oligoadenylates. The principal function of these products is to activate the latent RNase L, which in turn degrades viral and cellular single-stranded RNA (ssRNA). During its replication, rotavirus generates viral dsRNA as well as ssRNA with a double-stranded secondary structure. If the increase in mRNA of OAS1 detected in this analysis reflects an increase of this protein, we can suggest that the OAS1/RNase L system is a mechanism of cellular defense against rotavirus infection. The activation of PKR, another protein with an alternative antiviral effect by rotavirus dsRNA, has also been proposed (46).

Several previous reports suggested a possible role for IFNs in host defense against rotavirus infectious. In vitro, IFN-α, and IFN-γ pretreatment inhibits rotavirus entry into human intestinal cell lines (3). Rollo et al. found activation of the IFN-induced transcription factor ISGF3 in HT-29 cells, indicating that RRV infection induces a sustained production and action of IFN-α/β that begins a few hours after infection (46). In vivo, administration of IFN-α/β to pigs and calves diminished virus replication and diarrhea (35, 49), and high levels of IFN-α/β and the antiviral IFN-induced protein MxA were found in the peripheral blood cells of patients and animals infected with rotavirus (8–10, 33, 38). From these and our own findings it seems likely that rotavirus-infected cells efficiently activate the transcription of many IFN-induced genes to create an antiviral state. In contrast, studies to directly determine the importance of IFNs in modulating rotavirus disease and infection in vivo have shown that the lack of IFN did not augment the intensity of diarrhea or change the amount of virus shedding (1). Moreover, a previous report from our laboratory demonstrated that IFN-γ is not an essential mediator of the antirotavirus effect of $CD8^+$ T cells since IFN-γ knockout mice and mice depleted of IFNγ by administration of an anti-IFN-γ monoclonal antibody cleared rotavirus infection as efficiently as control mice (17).

The apparent discrepancy between the transcriptional activation of IFN-induced genes and the lack of a role of endogenous IFNs in the resolution of rotavirus disease and infection in the mouse model could be explained by the existence of a specific viral mechanism designed to blunt or eliminate the IFN response of the host cell. Different mechanisms of resistance to IFN effects have been reported in different viral systems. For example, Kaposi sarcoma-associated herpesvirus encodes a gene product that has homology to the IRF family of transcription factors and inhibits the response to IFN-α/β and IFN-γ (61). The dsRNA-binding protein NS1 of influenza A virus inhibits the activation of IRF3, presumably by sequestering double-stranded forms of RNA which could potentially activate IRF-3 and initiate the induction of an antiviral state (56). Others viruses, including adenovirus and Epstein-Barr virus, inhibit the IFN-induced PKR by a virus-encoded RNA that binds to PKR and impairs its activation by dsRNA (reviewed in reference 19). The activity of the OAS1/RNase L system is also target of inhibition by several viruses, such as EMCV and herpes simplex virus (51). Recently, was shown that the influenza B virus protein NS1 blocks the function of the IFN-inducible protein ISG15 (59). Since viruses have developed a variety of countermechanisms to block the antiviral response of IFNs, we speculate that rotavirus may also have developed an IFN-interfering mechanism to overcome host cell defense. The identification and characterization of such mechanisms warrants further investigation.

**Rotavirus infection and calcium homeostasis.** Several studies indicate that calcium is a critical factor in rotavirus cytopathology. On the one hand, this cation is required for rotavirus morphogenesis, while on the other hand calcium accumulation appears to be responsible for the cytopathic effect and cell death observed at late stages of infection. The alteration of calcium homeostasis during rotavirus infection has been directly related to the synthesis of specific viral proteins. Recent studies have found that the rotavirus nonstructural protein NSP4 increases the intracellular calcium concentration ($[Ca^{2+}]_i$) when expressed endogenously in Sf9 insect cells or when added exogenously to Sf9 or human intestinal HT-29 cells (13, 57). NSP4 has been shown to be an enterotoxin that induces diarrhea in young mice; the physiological evidence suggests that NSP4 activates a signal transduction pathway that increases $[Ca^{2+}]_i$ by mobilizing $Ca^{2+}$ from the ER and resulting in transepithelial chloride secretion (2).

In addition to the role of NSP4 in the changes in $[Ca^{2+}]_i$, del Castillo et al. and Perez et al. have found a progressive increase in plasma membrane permeability to mono and divalent cations a few hours after rotavirus infection (11, 44). The characterization of the $Ca^{2+}$ entry pathway suggests that rotavirus infection activates an L-type $Ca^{2+}$channel of the plasma membrane in MA104 and HT-29 cells (44). Interestingly, in this study we reported the upregulation of the alpha 1D subunit of this L-type calcium channel, supporting the involvement of this channel in the pathway of plasma membrane permeability observed during rotavirus infection.

The genes encoding for S100A3 and S100A8 were also upregulated. These proteins belong to a family of low-molecular-weight $Ca^{2+}$-binding proteins of the EF-hand type known as S100. Previous work has implicated S100 proteins in $Ca^{2+}$-dependent regulation of intracellular and extracellular functions such as protein phosphorylation, calcium homeostasis, inflammation, and regulation of the dynamics of cytoskeleton components (12).

The three major constituents of the cytoskeleton—microtubules, microfilaments, and intermediate filaments—are targets of S100 proteins (reviewed in reference 12). It is now well documented that members of this protein family inhibit tubulin polymerization and cause disassembly of preformed microtubules in the presence of micromolar concentrations of free $[Ca^{2+}]_i$. The S100A8/S100A9 complex modulates $Ca^{2+}$-de-

pendent interactions between vimentin, keratin intermediate filaments, and membranes. S100A2 plays a role in the organization of the actin cytoskeleton by regulating F actin-tropomyosin interactions in epithelial cell lines in a $Ca^{2+}$-dependent manner. It is interesting that the rotavirus-induced increases in $[Ca^{2+}]_i$ have been shown to be directly responsible for the disassembly of microvillar F-actin and the microtubule network in differentiated Caco-2 cells at late times after rotavirus infection (5, 6). If the increase in mRNA of S100A3 and S100A8 reported in this analysis reflects an increase of these proteins, it seems possible that these proteins participate in the $Ca^{2+}$-dependent disorganization of cytoskeleton observed in RRV-infected cells.

In summary, we have studied the relative abundance of more than 8,000 human transcripts in Caco-2 cells infected with rotavirus. We learned that 6.7% of the analyzable transcripts were regulated at 16 hpi, 73.4% of them being upregulated genes, and the majority of the changes observed occurred late after infection, primarily at or after 12 h. This global analysis provides a new picture of the cellular response to rotavirus infection. Although the relationships between cellular mRNA levels and the rotavirus replication cycle are not clear, further characterization of the response of individual genes can provide a better understanding of host-pathogen interaction. Future studies should also focus on which components of the virus replication cycle (binding, entry, transcription and translation, assembly, etc.) are responsible for the transcriptional changes observed, which viral genes mediate these changes and whether the transcriptional response program identified in this cell culture model is representative of changes seen in the intestine in vivo.

## ACKNOWLEDGMENTS

M.A.C. and D.A.F. contributed equally to this study.

This work was supported by a VA Merit Review grant, by NIH grants AI21362 and DK38707, and by DDC grant DK56339. Mariela A. Cuadras was on academic leave absence from the Instituto de Biotecnologia/UNAM, Cuernavaca, Morelos, Mexico, and was supported by an NIH-funded Emerging and Reemerging Infectious Disease fellowship (ID43TW00923).

We especially thank P. Brown and colleagues for technical advice and discussion.

## REFERENCES

1. **Angel, J., M. A. Franco, H. B. Greenberg, and D. Bass.** 1999. Lack of a role for type I and type II interferons in the resolution of rotavirus-induced diarrhea and infection in mice J. Interferon Cytokine Res. **19:**655–659.
2. **Ball, J. M., P. Tian, C. Q. Zeng, A. P. Morris, and M. K. Estes.** 1996. Age-dependent diarrhea induced by a rotaviral nonstructural glycoprotein Science **272:**101–104.
3. **Bass, D. M.** 1997. Interferon gamma and interleukin 1, but not interferon alpha, inhibit rotavirus entry into human intestinal cell lines. Gastroenterology **113:**81–89.
4. **Bishop, R. F., G. P. Davidson, I. H. Holmes, and B. J. Ruck.** 1973. Virus particles in epithelial cells of duodenal mucosa from children with acute non-bacterial gastroenteritis. Lancet **ii:**1281–1283.
5. **Brunet, J. P., J. Cotte-Laffitte, C. Linxe, A. M. Quero, M. Geniteau-Legendre, and A. Servin.** 2000. Rotavirus infection induces an increase in intracellular calcium concentration in human intestinal epithelial cells: role in microvillar actin alteration. J. Virol. **74:**2323–2332.
6. **Brunet, J. P., N. Jourdan, J. Cotte-Laffitte, C. Linxe, M. Geniteau-Legendre, A. Servin, and A. M. Quero.** 2000. Rotavirus infection induces cytoskeleton disorganization in human intestinal epithelial cells: implication of an increase in intracellular calcium concentration. J. Virol. **74:**10801–10806.
7. **Chang, Y. E., and L. A. Laimins.** 2000. Microarray analysis identifies interferon-inducible genes and Stat-1 as major transcriptional targets of human papillomavirus type 31. J. Virol. **74:**4174–4182.
8. **Chieux, V., D. Hober, W. Chehadeh, J. Harvey, G. Alm, J. Cousin, H. Ducoulombier, and P. Wattre.** 1999. MxA protein in capillary blood of children with viral infections. J. Med. Virol. **59:**547–551.
9. **Chieux, V., D. Hober, J. Harvey, G. Lion, D. Lucidarme, G. Forzy, M. Duhamel, J. Cousin, H. Ducoulombier, and P. Wattre.** 1998. The MxA protein levels in whole blood lysates of patients with various viral infections. J. Virol. Methods **70:**183–191.
10. **De Boissieu, D., P. Lebon, J. Badoual, Y. Bompard, and C. Dupont.** 1993. Rotavirus induces alpha-interferon release in children with gastroenteritis. J. Pediatr. Gastroenterol. Nutr. **16:**29–32.
11. **del Castillo, J. R., J. E. Ludert, A. Sanchez, M. C. Ruiz, F. Michelangeli, and F. Liprandi.** 1991. Rotavirus infection alters $Na^+$ and $K^+$ homeostasis in MA-104 cells. J. Gen. Virol. **72:**541–547.
12. **Donato, R.** 1999. Functional roles of S100 proteins, calcium-binding proteins of the EF-hand type. Biochim. Biophys. Acta **1450:**191–231.
13. **Dong, Y., C. Q. Zeng, J. M. Ball, M. K. Estes, and A. P. Morris.** 1997. The rotavirus enterotoxin NSP4 mobilizes intracellular calcium in human intestinal cells by stimulating phospholipase C-mediated inositol 1,4,5-trisphosphate production. Proc. Natl. Acad. Sci. USA **94:**3960–3965.
14. **Eisen, M. B., P. T. Spellman, P. O. Brown, and D. Botstein.** 1998. Cluster analysis and display of genome-wide expression patterns. Proc. Natl. Acad. Sci. USA **95:**14863–14868.
15. **Estes, M. K.** 2001. Rotaviruses and their replication, p. 1747–1786. *In* B. N. Fields, D. M. Knipe, and P. M. Howley (ed.), Fields virology, 4th ed., vol. 2. Lippincott/The Williams & Wilkins Co., Philadelphia, Pa.
16. **Fogh, J., J. M. Fogh, and T. Orfeo.** 1977. One hundred and twenty-seven cultured human tumor cell lines producing tumors in nude mice. J. Natl. Cancer Inst. **59:**221–226.
17. **Franco, M. A., C. Tin, L. S. Rott, J. L. VanCott, J. R. McGhee, and H. B. Greenberg.** 1997. Evidence for $CD8^+$ T-cell immunity to murine rotavirus in the absence of perforin, fas, and gamma interferon. J. Virol. **71:**479–486.
18. **Fukudome, K., O. Yoshie, and T. Konno.** 1989. Comparison of human, simian, and bovine rotaviruses for requirement of sialic acid in hemagglutination and cell adsorption. Virology **172:**196–205.
19. **Gale, M., Jr., and M. G. Katze.** 1998. Molecular mechanisms of interferon resistance mediated by viral-directed inhibition of PKR, the interferon-induced protein kinase. Pharmacol Ther. **78:**29–46.
20. **Geiss, G. K., M. C. An, R. E. Bumgarner, E. Hammersmark, D. Cunningham, and M. G. Katze.** 2001. Global impact of influenza virus on cellular pathways is mediated by both replication-dependent and -independent events. J. Virol. **75:**4321–4331.
21. **Geiss, G. K., R. E. Bumgarner, M. C. An, M. B. Agy, A. B. van 't Wout, E. Hammersmark, V. S. Carter, D. Upchurch, J. I. Mullins, and M. G. Katze.** 2000. Large-scale monitoring of host cell gene expression during HIV-1 infection using cDNA microarrays. Virology **266:**8–16.
22. **Glass, R. I., J. R. Gentsch, and B. Ivanoff.** 1996. New lessons for rotavirus vaccines. Science **272:**46–48.
23. **Guerrero, C. A., D. Bouyssounade, S. Zarate, P. Isa, T. Lopez, R. Espinosa, P. Romero, E. Mendez, S. Lopez, and C. F. Arias.** 2002. Heat shock cognate protein 70 is involved in rotavirus cell entry. J. Virol. **76:**4096–4102.
24. **Guerrero, C. A., E. Mendez, S. Zarate, P. Isa, S. Lopez, and C. F. Arias.** 2000. Integrin $\alpha_v\beta_3$ mediates rotavirus cell entry. Proc. Natl. Acad. Sci. USA **97:**14644–14649.
25. **Heath, R. L., and C. J. Birch.** 1988. Synthesis of human rotavirus polypeptides in cell culture. J. Med. Virol. **25:**91–103.
26. **Hewish, M. J., Y. Takada, and B. S. Coulson.** 2000. Integrins $\alpha_2\beta_1$ and $\alpha_4\beta_1$ can mediate SA11 rotavirus attachment and entry into cells. J. Virol. **74:**228–236.
27. **Iyer, V. R., M. B. Eisen, D. T. Ross, G. Schuler, T. Moore, J. C. Lee, J. M. Trent, L. M. Staudt, J. Hudson, Jr., M. S. Boguski, D. Lashkari, D. Shalon, D. Botstein, and P. O. Brown.** 1999. The transcriptional program in the response of human fibroblasts to serum. Science **283:**83–87.
28. **Jourdan, N., J. P. Brunet, C. Sapin, A. Blais, J. Cotte-Laffitte, F. Forestier, A. M. Quero, G. Trugnan, and A. L. Servin.** 1998. Rotavirus infection reduces sucrase-isomaltase expression in human intestinal epithelial cells by perturbing protein targeting and organization of microvillar cytoskeleton. J. Virol. **72:**7228–7236.
29. **Jourdan, N., M. Maurice, D. Delautier, A. M. Quero, A. L. Servin, and G. Trugnan.** 1997. Rotavirus is released from the apical surface of cultured human intestinal cells through nonconventional vesicular transport that bypasses the Golgi apparatus. J. Virol. **71:**8268–8278.
30. **Kapikian, A. Z., Y. Hoshino, and R. M. Chanock.** 2001. Rotaviruses, p. 1787–1834. *In* B. N. Fields, D. M. Knipe, and P. M. Howley (ed.), Fields virology, 4th ed., vol. 2. Lippincott/The Williams & Wilkins Co., Philadelphia, Pa.
31. **Keljo, D. J., and A. K. Smith.** 1988. Characterization of binding of simian rotavirus SA-11 to cultured epithelial cells. J. Pediatr. Gastroenterol. Nutr. **7:**249–256.
32. **Kitamoto, N., R. F. Ramig, D. O. Matson, and M. K. Estes.** 1991. Comparative growth of different rotavirus strains in differentiated cells (MA104, HepG2, and CaCo-2). Virology **184:**729–737.
33. **La Bonnardiere, C., J. Cohen, and M. Contrepois.** 1981. Interferon activity in rotavirus infected newborn calves. Ann. Rech. Vet. **12:**85–91.

34. **Lama, J., A. Mangasarian, and D. Trono.** 1999. Cell-surface expression of CD4 reduces HIV-1 infectivity by blocking Env incorporation in a Nef- and Vpu-inhibitable manner. Curr. Biol. **9:**622–631.
35. **Lecce, J. G., J. M. Cummins, and A. B. Richards.** 1990. Treatment of rotavirus infection in neonate and weanling pigs using natural human interferon alpha. Mol. Biother. **2:**211–216.
36. **Lennon, G., C. Auffray, M. Polymeropoulos, and M. B. Soares.** 1996. The I.M.A.G.E. Consortium: an integrated molecular analysis of genomes and their expression. Genomics **33:**151–152.
37. **Lizano, M., S. Lopez, and C. F. Arias.** 1991. The amino-terminal half of rotavirus SA114fM VP4 protein contains a hemagglutination domain and primes for neutralizing antibodies to the virus. J. Virol. **65:**1383–1391.
38. **Mangiarotti, P., F. Moulin, P. Palmer, S. Ravilly, J. Raymond, and D. Gendrel.** 1999. Interferon-alpha in viral and bacterial gastroenteritis: a comparison with C-reactive protein and interleukin-6. Acta Paediatr. **88:**592–594.
39. **Menard, R., C. Dehio, and P. J. Sansonetti.** 1996. Bacterial entry into epithelial cells: the paradigm of *Shigella*. Trends Microbiol. **4:**220–226.
40. **Mengaud, J., H. Ohayon, P. Gounon, R. M. Mege, and P. Cossart.** 1996. E-cadherin is the receptor for internalin, a surface protein required for entry of *L. monocytogenes* into epithelial cells. Cell **84:**923–932.
41. **Michelangeli, F., F. Liprandi, M. E. Chemello, M. Ciarlet, and M. C. Ruiz.** 1995. Selective depletion of stored calcium by thapsigargin blocks rotavirus maturation but not the cytopathic effect. J. Virol. **69:**3838–3847.
42. **Morgan, R. W., L. Sofer, A. S. Anderson, E. L. Bernberg, J. Cui, and J. Burnside.** 2001. Induction of host gene expression following infection of chicken embryo fibroblasts with oncogenic Marek's disease virus. J. Virol. **75:**533–539.
43. **Obert, G., I. Peiffer, and A. L. Servin.** 2000. Rotavirus-induced structural and functional alterations in tight junctions of polarized intestinal Caco-2 cell monolayers. J. Virol. **74:**4645–4651.
44. **Perez, J. F., M. C. Ruiz, M. E. Chemello, and F. Michelangeli.** 1999. Characterization of a membrane calcium pathway induced by rotavirus infection in cultured cells. J. Virol. **73:**2481–2490.
45. **Piron, M., P. Vende, J. Cohen, and D. Poncet.** 1998. Rotavirus RNA-binding protein NSP3 interacts with eIF4GI and evicts the poly(A) binding protein from eIF4F. EMBO J. **17:**5811–5821.
46. **Rollo, E. E., K. P. Kumar, N. C. Reich, J. Cohen, J. Angel, H. B. Greenberg, R. Sheth, J. Anderson, B. Oh, S. J. Hempson, E. R. Mackow, and R. D. Shaw.** 1999. The epithelial cell response to rotavirus infection. J. Immunol. **163:**4442–4452.
47. **Samuel, C. E.** 1991. Antiviral actions of interferon. Interferon-regulated cellular proteins and their surprisingly selective antiviral activities. Virology **183:**1–11.
48. **Schena, M., D. Shalon, R. W. Davis, and P. O. Brown.** 1995. Quantitative monitoring of gene expression patterns with a complementary DNA microarray. Science **270:**467–470.
49. **Schwers, A., C. Vanden Broecke, M. Maenhoudt, J. M. Beduin, J. Werenne, and P. P. Pastoret.** 1985. Experimental rotavirus diarrhoea in colostrum-deprived newborn calves: assay of treatment by administration of bacterially produced human interferon (Hu-IFN $\alpha$ 2). Ann. Rech. Vet. **16:**213–218.
50. **Sen, G. C.** 2000. Novel functions of interferon-induced proteins. Semin. Cancer Biol. **10:**93–101.
51. **Sen, G. C., and P. Lengyel.** 1992. The interferon system. A bird's eye view of its biochemistry. J. Biol. Chem. **267:**5017–5020.
52. **Sherlock, G., T. Hernandez-Boussard, A. Kasarskis, G. Binkley, J. C. Matese, S. S. Dwight, M. Kaloper, S. Weng, H. Jin, C. A. Ball, M. B. Eisen, P. T. Spellman, P. O. Brown, D. Botstein, and J. M. Cherry.** 2001. The Stanford Microarray Database. Nucleic Acids Res. **29:**152–155.
53. **Stark, G. R., I. M. Kerr, B. R. Williams, R. H. Silverman, and R. D. Schreiber.** 1998. How cells respond to interferons. Annu. Rev. Biochem. **67:**227–264.
54. **Stein, M. A., D. A. Mathers, H. Yan, K. G. Baimbridge, and B. B. Finlay.** 1996. Enteropathogenic *Escherichia coli* markedly decreases the resting membrane potential of Caco-2 and HeLa human epithelial cells. Infect. Immun. **64:**4820–4825.
55. **Svensson, L., B. B. Finlay, D. Bass, C. H. von Bonsdorff, and H. B. Greenberg.** 1991. Symmetric infection of rotavirus on polarized human intestinal epithelial (Caco-2) cells. J. Virol. **65:**4190–4197.
56. **Talon, J., C. M. Horvath, R. Polley, C. F. Basler, T. Muster, P. Palese, and A. Garcia-Sastre.** 2000. Activation of interferon regulatory factor 3 is inhibited by the influenza A virus NS1 protein. J. Virol. **74:**7989–7996.
57. **Tian, P., Y. Hu, W. P. Schilling, D. A. Lindsay, J. Eiden, and M. K. Estes.** 1994. The nonstructural glycoprotein of rotavirus affects intracellular calcium levels. J. Virol. **68:**251–257.
58. **Xu, A., A. R. Bellamy, and J. A. Taylor.** 1998. BiP (GRP78) and endoplasmin (GRP94) are induced following rotavirus infection and bind transiently to an endoplasmic reticulum-localized virion component. J. Virol. **72:**9865–9872.
59. **Yuan, W., and R. M. Krug.** 2001. Influenza B virus NS1 protein inhibits conjugation of the interferon (IFN)-induced ubiquitin-like ISG15 protein. EMBO J. **20:**362–371.
60. **Zhu, H., J. P. Cong, G. Mamtora, T. Gingeras, and T. Shenk.** 1998. Cellular gene expression altered by human cytomegalovirus: global monitoring with oligonucleotide arrays. Proc. Natl. Acad. Sci. USA **95:**14470–14475.
61. **Zimring, J. C., S. Goodbourn, and M. K. Offermann.** 1998. Human herpesvirus 8 encodes an interferon regulatory factor (IRF) homolog that represses IRF-1-mediated transcription. J. Virol. **72:**701–707.
62. **Zweibaum, A., N. Triadou, M. Kedinger, C. Augeron, S. Robine-Leon, M. Pinto, M. Rousset, and K. Haffen.** 1983. Sucrase-isomaltase: a marker of foetal and malignant epithelial cells of the human colon. Int. J. Cancer **32:**407–412.